water

MDPI

*Article*

# Application of Water Quality Indices, Machine Learning Approaches, and GIS to Identify Groundwater Quality for Irrigation Purposes: A Case Study of Sahara Aquifer, Doucen Plain, Algeria

**Aissam Gaagai [1,*], Hani Amir Aouissi [1,2,3], Selma Bencedira [4], Gilbert Hinge [5], Ali Athamena [6], Salim Haddam [7], Mohamed Gad [8,*], Osama Elsherbiny [9], Salah Elsayed [10,*], Mohamed Hamdy Eid [11,12] and Hekmat Ibrahim [13]**

1 Scientific and Technical Research Center on Arid Regions (CRSTRA), Biskra 07000, Algeria
2 Environmental Research Center (CRE), Badji Mokhtar Annaba University, Annaba 23000, Algeria
3 Laboratoire de Recherche et d'Etude en Aménagement et Urbanisme (LREAU), Université des Sciences et de la Technologie (USTHB), Algiers 16000, Algeria
4 Laboratory of LGE, Department of Process Engineering, Faculty of Technology, University Badji-Mokhtar Annaba, Annaba 23000, Algeria
5 Department of Civil Engineering, National Institute of Technology Durgapur, Durgapur 713209, India
6 Department of Geology, Institute of Earth and Universe Sciences, University of Batna 2, Fesdis 05078, Algeria
7 Agronomy Department, Faculty of Science, Hydraulic Division University, 20 Août 1955, Skikda 21000, Algeria
8 Hydrogeology, Evaluation of Natural Resources Department, Environmental Studies and Research Institute, University of Sadat City, Minufiya 32897, Egypt
9 Agricultural Engineering Department, Faculty of Agriculture, Mansoura University, Mansoura 35516, Egypt
10 Agricultural Engineering, Evaluation of Natural Resources Department, Environmental Studies and Research Institute, University of Sadat City, Minufiya 32897, Egypt
11 Institute of Environmental Management, Faculty of Earth Science, University of Miskolc, Egyetemváros, 3515 Miskolc, Hungary
12 Geology Department, Faculty of Science, Beni-Suef University, Beni-Suef 65211, Egypt
13 Geology Department, Faculty of Science, Menoufia University, Shiben El Kom 51123, Minufiya, Egypt
* Correspondence: gaagaiaissam37@gmail.com (A.G.); mohamed.gad@esri.usc.edu.eg (M.G.); salah.emam@esri.usc.edu.eg (S.E.)

check for updates

**Citation:** Gaagai, A.; Aouissi, H.A.; Bencedira, S.; Hinge, G.; Athamena, A.; Haddam, S.; Gad, M.; Elsherbiny, O.; Elsayed, S.; Eid, M.H.; et al. Application of Water Quality Indices, Machine Learning Approaches, and GIS to Identify Groundwater Quality for Irrigation Purposes: A Case Study of Sahara Aquifer, Doucen Plain, Algeria. *Water* **2023**, *15*, 289. https://doi.org/10.3390/w15020289

Academic Editor: Chin H. Wu

Received: 8 December 2022
Revised: 5 January 2023
Accepted: 7 January 2023
Published: 10 January 2023



**Abstract:** In order to evaluate and project the quality of groundwater utilized for irrigation in the Sahara aquifer in Algeria, this research employed irrigation water quality indices (IWQIs), artificial neural network (ANN) models, and Gradient Boosting Regression (GBR), alongside multivariate statistical analysis and a geographic information system (GIS), to assess and forecast the quality of groundwater used for irrigation in the Sahara aquifer in Algeria. Twenty-seven groundwater samples were examined using conventional analytical methods. The obtained physicochemical parameters for the collected groundwater samples showed that $Ca^{2+} > Mg^{2+} > Na^{+} > K^{+}$, and $Cl^{-} > SO_4{}^{2-} > HCO_3{}^{-} > NO_3{}^{-}$, owing to the predominance of limestone, sandstone, and clay minerals under the effects of human activity, ion dissolution, rock weathering, and exchange processes, which indicate a Ca-Cl water type. For evaluating the quality of irrigation water, the IWQIs values such as irrigation water quality index (IWQI), sodium adsorption ratio (SAR), Kelly index (KI), sodium percentage (Na%), permeability index (PI), and magnesium hazard (MH) showed mean values of 47.17, 1.88, 0.25, 19.96, 41.18, and 27.87, respectively. For instance, the IWQI values revealed that 33% of samples were severely restricted for irrigation, while 67% of samples varied from moderate to high restriction for irrigation, indicating that crops that are moderately to highly hypersensitive to salt should be watered in soft soils without any compressed layers. Two-machine learning models were applied, i.e., the ANN and GBR for IWQI, and the ANN model, which surpassed the GBR model. The findings showed that ANN-2F had the highest correlation between IWQI and exceptional features, making it the most accurate prediction model. For example, this model has two qualities that are critical for the IWQI prediction. The outputs' $R^2$ values for the training and validation sets are 0.973 (RMSE = 2.492) and 0.958 (RMSE = 2.175), respectively. Finally, the application of physicochemical parameters and water quality indices supported by GIS methods, machine learning, and multivariate modeling is a useful and practical strategy for evaluating the quality and development of groundwater.

**Keywords:** geographic information system (GIS); artificial neural network (ANN); multivariate analysis; gradient boosting regression (GBR); Sahara aquifer; Algeria

## 1. Introduction

Groundwater is a crucial source of freshwater for humans. However, with enormous population growth, agricultural use, industrialization, and unplanned urbanization, the extraction of groundwater has continuously increased from 283 $km^3$/year in the 1960s to more than 700 $km^3$/year in the last decades [1]. In many parts of the world, excessive groundwater extraction threatens both the amount and quality of water by causing dramatic drops in the water tables. Groundwater quality is essential in determining whether it is acceptable for use in agriculture and other industries. Numerous elements, like the makeup of the soil, seasonal variations, hydrogeochemical practices, and human actions, have an influence on the quality of groundwater [2–6].

In recent years, the deterioration of groundwater quality has been exacerbated by uncontrolled leaching of leachate from landfills, excessive use of fertilizers, and other human activities that are significantly dangerous to human health [7–10]. Many studies have evaluated groundwater quality in the world [11,12]. Nevertheless, the majority of these studies primarily concentrated on single-parameter evaluation, in which the governing elements were assessed individually, and the most compromised factor had a significant influence on water quality [13]. Hence, there is an increasing need for techniques that allow for better water quality interpretation to ensure effective groundwater quality control and management. Owing to their statistical ease of use and adaptability. Irrigation water quality indices (IWQIs) are among the best methods for monitoring groundwater quality for agricultural activities. IWQIs can help to interpret complex water quality data in simple terms [14–16]. Several indices have been used to categorize groundwater quality for agricultural purposes. These indices include the irrigation water quality index (IWQI), permeability index (PI), sodium adsorption ratio (SAR), Kelly index (KI), magnesium hazard (MH), and sodium percentage (Na%) [17].

Additionally, researchers' interest in the application of multivariate statistical methods, such as principal component analysis (PCA) and cluster analysis (CA), as well as geographic information system (GIS) analysis, has grown [18], particularly in the assessment of water quality [19]. Multivariate statistical approaches and GIS analysis have been utilized collaboratively to highlight the primary variables affecting the geographical distribution of groundwater quality. For example, Nas and Berktay [20] used GIS and traditional kriging to analyze the spatial variation of groundwater quality indicators and map groundwater quality in urban areas in Konya, Turkey. Gilbert et al. [21] used a combination of GIS and multivariate analysis to analyze groundwater distribution in India. Studies conducted in multiple nations, including the United States, and India, revealed that groundwater found in various geological settings exhibits a variety of hydrochemical properties and falls into a few graded categories of water intended for irrigation [14–16,22–26].

In addition, by assigning weights to important ions based on entropy, researchers have explored approaches to reduce the subjectivity of existing water quality index technology, which has been displayed to be a more precise and vital method for precise weighing systems [27]. Water quality research, on the other hand, necessitates a significant amount of data collection, laboratory analysis, data management, and testing [28]. As a result of the computation's subjectivity, WQI's interpretation of the findings contains inconsistencies. According to previous studies, there is not a perfect WQI model. Consequently, it is crucial to implement a workable and affordable plan for accurate water quality assessment. Further, techniques for selecting features based on models [29] can be used to isolate a subset of features that have a predictive and a high discriminative. This method can improve model performance by reducing over-fitting and deleting unnecessary features. In addition to enhancing interpretability, retaining the original feature representation has its own set of advantages [30]. Moreover, there is a growing demand for feature selection algorithms in the fields of modeling and prediction [31]. Numerous researchers have investigated the effectiveness of various methods, such as Gradient Boosting Regression (GBR), Decision Tree (DT), and Random Forest (RF), for reducing the dimensionality of data. The RF model ranks all factors in terms of their importance [32]. Glorfeld [33] created a back-propagation neural network index to recognize the most important elements. In addition, the picking of hyperparameters has numerous benefits and can greatly affect the performance of any machine learning model. It could, for instance, boost ML algorithm performance [34] or make scientific studies more equitable and reproducible [35]. Given its potential significance in bettering the prediction model [36], it has a direct impact on how training algorithms act.

The groundwater of the Doucen plain is confined to the Sahara aquifers in the Northwestern region of Ouled Djelal, Algeria. It is exposed to varying degrees of salinity, which is attributed to the underlying fresh groundwater horizon, various pollutants of anthropogenic origin, and connate water trapped in aquifer rocks. However, to the best of the author's knowledge, no comprehensive water quality research has been conducted on the Doucen plain. Physicochemical parameters focused on hydrochemical features offer preliminary knowledge regarding water facies, various geochemical pathways, and water classification [17,37]. Therefore, this study aims to (i) identify the groundwater characteristics, groundwater facies, and geochemical controlling mechanisms using physicochemical parameters, Chloro-alkaline indices (CAI 1 and CAI 2), multiple graphical approaches, and multivariate statistical analysis, (ii) assess and classify the groundwater quality for irrigation using IWQIs and (iii) assess the performance of ANN and GBR models to forecast the six IWQIs, namely IWQI, SAR, KI, Na%, MH, and PI.

## 2. Materials and Methods

### 2.1. Study Area

The region of Doucen is located in the Northwestern city ("wilaya") of Ouled Djelal (Figure 1). The plain of Doucen extends over almost 12.42 miles from the wilaya of Ouled Djelal and 49.70 miles from the capital of the Biskra Provence. It is located at an elevation of over 102 m and between 4°57′ and 5°17′ east longitude and 34°30′ and 34°45′ north latitude. Area-wise, it's 247.87 square miles, and it has administrative borders with the communes of Chaiba to the west, El-Ghrouss to the east and north, the town of Ouled Djalel to the south, the commune of Lioua to the east, and the commune of Still (El Oued willaya) to the south-east. It is an oasis with a strong agricultural vocation that mainly produces dates but also melons and watermelons. The commune of Doucen is vast, and it brings together several urbanized centers; the most important ones are "Doucen Ville" and "Tafechna".

Geologically, the Doucen region consists of formations of ages ranging from Secondary to Quaternary. Secondary formations (Cretaceous) consist of limestone, crystalline limestone, dolomites, sandstone, gypsum, anhydrite, clays, and marls, while tertiary formations (Paleogene and Neogene) consist of limestone, marls, gypsum, clays, gravel, and sand red. The quaternary formations consist of scree, pebbles, gravel, sand, gypsum limestone, sandy alluvium, and clay alluvium (Figure 2). Hydrogeological studies have made it possible to highlight the existence of several aquifer reservoirs of distinct importance in terms of their lithological constitution, their geological structure, and the ease with which they are exploited (Figure S1).

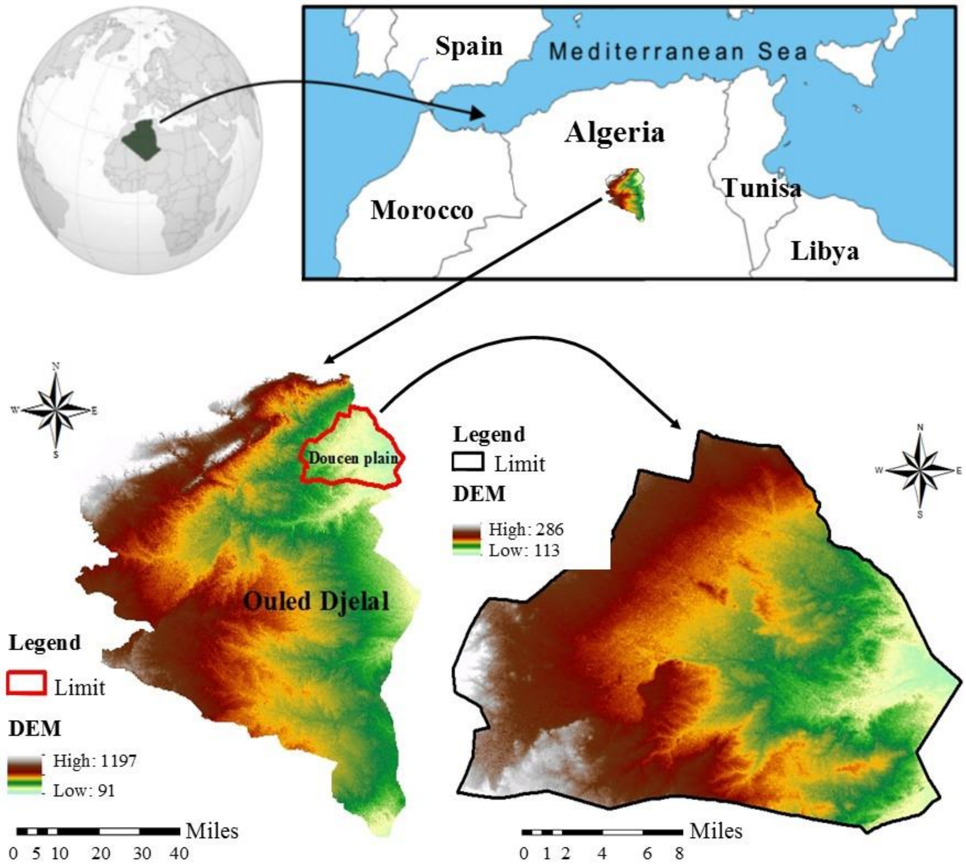


**Figure 1.** Map of the study area (Doucen plain, Algeria).

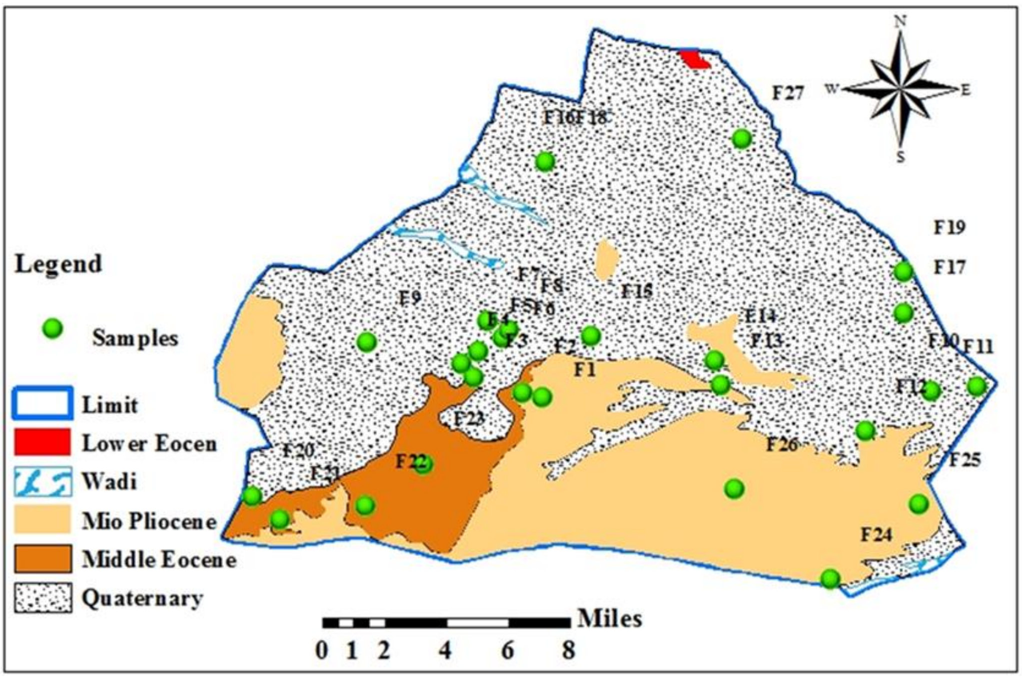


**Figure 2.** Geological map of the Doucen plain, Algeria.

### 2.2. Sampling and Hydrochemistry

#### 2.2.1. Samples Collection

Twenty-seven (27) samples were collected from the study region (Figure 2). The positions of the sample stations were recorded using a global positioning system (GPS map, 76 CSx). During and after the wet season, contaminants are likely to be susceptible to seeping downhill [38]. Thus, water was pumped out for approximately 15 min before sampling to eliminate stagnant water. The samples were collected using polypropylene (PP) bottles, as proposed in a previous study [39]. Then, 0.45-µm acetate cellulose filters were employed to clean the samples. In the absence of acidification, 250 $cm^3$ PE bottles were used for collecting samples for anions analysis. At last, the Algerian Waters laboratory in Biskra received the samples that had been kept at a temperature of <4 °C (The laboratory is accredited under ISO/IEC 17025).

#### 2.2.2. Measurement of the Physicochemical Parameters

A WTW multiparameter (Weilheim, Germany) was used to monitor the physicochemical parameters (pH, temperature, and electric conductivity). Titration was employed to compute the concentrations of $Ca^{2+}$, $Mg^{2+}$, $Cl^-$, and $HCO_3^-$ ions. The value of $SO_4^{2-}$ was found by employing spectrophotometry. In addition, a flame photometer was utilized in order to perform analyses on the $K^+$ and $Na^+$. TDS concentration was determined by weighing and drying at 103–105 °C in an oven. Nitrates were determined using the cadmium column reduction method. With an analytical uncertainty of less than 4%, all samples were examined in triplicate (Source: Gore, Michael. Spectrophotometry & Spectrofluorimetry. New York: Oxford University Press, 2000). The cations-anions balance was initially checked to make sure it was within 5%, which helped decide the analysis' dependability by using recommended techniques from the American Public Health Association (APHA) [40]. The cadmium reduction method is a colorimetric method that involves contact of the nitrate in the sample with cadmium particles, which causes nitrates to be converted to nitrites. Hydrochemical outcomes were statistically investigated using DIAGRAMMES (version 5.8.0). STATISTICA software (version 8.0) was used to generate the results of the time series analysis and multivariate statistics.

#### 2.2.3. Multivariate Statistical Analysis for Data Treatment

Large datasets can be streamlined and organized using multivariate statistical approaches to produce valuable insights [41,42]. In our case, two multivariate statistical methods, Viz. Cluster analysis (CA) and Principal component analysis (PCA) were applied to evaluate the physicochemical variables of our groundwater samples. Using a suite of multivariate techniques, cluster analysis can identify meaningful classes within a dataset. Unlike the non-hierarchical method, the hierarchical approach to CA does not require the entire number of clusters to be known in advance. According to a survey conducted by Belkhiri et al. [43], Ward's method is superior to others because it results in a larger proportion of correctly identified observations. Thus, the present study adopts Ward's clustering method, and the Euclidean distance was used in the current work to apply CA [44]. Minimal information loss was achieved by data reduction and the extraction of the most important components using PCA [44]. The aim of this project was to conduct the principal components analysis (PCA) method to extract the major elements related to the various causes of variance in hydrochemical data collected from the Doucen plain because PCA is used by Ridley. However, specifics were not shared [45].

### *2.3. Indexing Approaches*

#### 2.3.1. Chloro-Alkaline Indices (CAI 1 and CAI 2)

Multiple ionic connections were employed to assess the dynamic geochemical procedures in the current investigation. It comprises the dealings of $[Ca^{2+} + Mg^{2+}]$ vs. $[SO_4^{2-} + HCO_3^-]$, $[Ca^{2+} + Mg^{2+}]$ vs. $[HCO_3^-]$, $[Ca^{2+}/Na^+]$ vs. $[Mg^{2+}/Na^+]$, $[HCO_3^-/Na^+]$ vs. $[Ca^{2+}/Mg^{2+}]$ and $[Na^+]$ vs. $[Cl^-]$. In addition, Equations (1) and (2) [46] were utilized to determine the ion exchange processes in the shallow aquifer using the Chloro-alkaline indices (CAI 1 and CAI 2):

$$\text{CAI 1} = \frac{Cl^- - (Na^+ + K^{+})}{Cl^-} \tag{1}$$

$$\mathrm{CAI\ 2} = \frac{\mathrm{Cl^- - (Na^+ + K^+)}}{\mathrm{SO_4^{2-} + HCO_3^- + CO_3^{2-} + NO_3^-}} \tag{2}$$

2.3.2. Irrigation Water Quality Indices (IWQIs)

According to Table 1, the IWQI, SAR, KI, Na%, MH, and PI% were all determined depended on the physicochemical parameters of the samples.

**Table 1.** The IWQIs, related formula and reference.

| WQIs | Formula | References |
|---|---|---|
| IWQI | $\sum_{i=1}^{n} \mathrm{Q_i W_i}$ | [47] |
| SAR | $\frac{\mathrm{Na^+}}{\sqrt{(\mathrm{Ca^{2+}+Mg^{2+}})/2}}$ | [48] |
| KI | $\frac{\mathrm{Na^+}}{\mathrm{Ca^{2+}+Mg^{2+}}}$ | [49] |
| Na% | $\frac{(\mathrm{Na^+ + K^+})}{(\mathrm{Ca^{2+}+Mg^{2+}})+(\mathrm{Na^+ + K^+})} \times 100$ | [50] |
| MH | $\left[\mathrm{Mg^{2+}}/\left(\mathrm{Ca^{2+} + Mg^{2+}}\right)\right] \times 100$ | [51] |
| PI | $\left(\frac{\mathrm{Na^+} + \sqrt{\mathrm{HCO_3^-}}}{(\mathrm{Ca^{2+}+Mg^{2+}+Na^+})}\right) \times 100$ | [52] |

Note(s): All IWQIs are calculated in meq/L.

*2.4. Spatial Distribution Pattern*

GIS are important tools for the analysis and performance of spatial data associated with groundwater source control. Our topographic map was digitized using the USGS satellite and ArcGIS software (ver. 10.5.x) for the preparation of the base map of the study area. Garmin GPSMAP 64sx was used to pinpoint the precise locations of the sampling spots (i.e., bore hole locations) using the GIS platform. Using ArcGIS 10.5 software, we were able to produce maps presenting the geographical distribution of groundwater quality indicators, such as IWQI, SAR, KI, Na%, MH, and PI%, that are useful for irrigation.

*2.5. Gradient Boosting Regression (GBR)*

Decision trees are the building blocks of GBR and can be utilized for either regression or classification. A set of trees was constructed, with each tree focusing on the prediction residuals of the previous tree [53]. GBR's hyperparameter tuning flexibility and ability to optimize a broad range of loss functions make it a highly flexible function-fitting technique. No pre-processing of the data is required, and it may be used for both numerical and categorical information. In addition, GBR can handle missing data on a large timescale. Simple trees are constructed in each iteration to prevent overfitting, and these can be used to extrapolate to novel data sets with greater precision. In general, a boosting approach has three parts: an additive model, some form of weak learners, and some type of loss function. The technique uses differentiable loss functions, can learn organically between input parameters over time, and can portray non-linear connections such as wind power curves [21]. To overcome the shortcomings of the underdeveloped models, gradient boosting machines are used to analyze gradients. To do this, we employ an iterative technique in which we unite base learners to decrease forecasting errors. Specifically, we use an additive model to combine decision trees and then employ gradient descent to decrease the loss function. The GBT (gradient boosting tree) $F_n(x_t)$ can be stated as the summation of $n$ regression-trees (Equations (3) and (4)).

$$F_n(x_t) = \sum_{i=1}^{n} f_i(x_t) \tag{3}$$

where every $f_i(x_t)$ is a decision tree (regression-tree). The ensemble of trees is constructed sequentially by estimating $f_{n+1}(x_t)$ which is the new decision tree, using the following equation:

$$argmin \sum_t L(y_t.F_n(x_t) + f_{n+1}(x_t)) \quad (4)$$

where $L(.)$ is differentiable for loss-function $L(.)$. A steepest descent method is used to solve it.

During GBR training, two criteria were considered: the number of boosting stages to perform (Ns) and the number of features to consider when looking for the best split (Mf). For Ns and Mf, the parameter values were (5,10, 15, 20, 25) and ('auto', 'sqrt', 'log2'), respectively. Then, hyper-parameter optimization was performed, and the top-level model was built using the best values.

### *2.6. Back-Propagation Neural Network (BPNN)*

The backpropagation neural network (BPNN) model is extremely popular [54]. There are three different types of layers that make up a BPNN: (1) the input layer, which serves as the neural net's primary data source; (2) the concealed layer, which acts as a bridge between the independent inputs layer and the dependent output layer; and (3) the final layer, which outputs the results of the inputs that were given. Artificial neural networks (ANNs) are a layer-by-layer machine learning approach for extracting high-level features from unstructured data. The number of nodes in the network is proportional to how well the regression works, while the network itself contains a hidden layer. The hidden layers nodes contain a set of parameters, which are typically referred to as weight and biases, which are what constitute the "updated parameters" in the network. "Output layer" refers to the final layer, and it shows the estimated value of the target variables. By adopting a network of neurons or nodes connected by weighted connections, ANN models are instances of generalized mathematical modeling that replicate the human brain in pattern detection and prediction [55,56].

During training, the network was subjected to no fewer than 2000 iterations or until the error measurement was less than $10^{-4}$. In order to train the model and determine the optimal number of neurons (3, 6, 9, 12, 15, 18, and 21) for the model's hidden layer, the validation strategy was combined with the LOOV technique. During the development of the ANN model, we investigated which activation function—"identity", "logistic", "tanh", and "relu"—was the most effective. The restriction imposed by memory to efficiently implement the technique, the weight optimizer Broyden-Fletcher-Goldfarb-Shanno (lbfgs), was employed [57]. The most important feature has to be identified so that the regression model's capacity for prediction may be increased and the complexity of hyperspectral images can be reduced [33,58].

### *2.7. Datasets and Software for Data Analysis*

In this study, 27 samples were used across the training and validation processes. The model was trained and verified with the use of a technique known as leave-one-out cross-validation (LOOCV). In each experiment, LOOCV will keep most of the data for training purposes while setting aside a subset for validation. This approach may mitigate the effects of over-fitting and yield a more precise measure of the model's prediction ability [59]. The software Python 3.7.3 was utilized for all these processes: data analysis, model construction, and data preparation. To perform tasks involving regression, the GBR and the ANN modules contained in the Scikit-learn package (version 0.20.2) were studied. A computer with an Intel Core i7-3630QM CPU running at a frequency of 2.4 GHz and 8 GB of Random Access Memory (RAM) was used for the data analysis.

### *2.8. Model Evaluation*

The effectiveness of a regression model has been evaluated using the following statistical measures: the coefficient of determination ($R^2$) and the root mean square error (RMSE) [60,61].

## 3. Results and Discussion

### *3.1. Groundwater Hydrochemical Properties*

The analysis of the local elemental molar concentrations reveals that the cations evolved as follows: $Ca^{2+} > Mg^{2+} > Na^{+} > K^{+}$ while the anions evolve in the following manner: $Cl^{-} > SO_4^{2-} > HCO_3^{-} > NO_3^{-}$. The distribution of the main ions ($Ca^{2+}$, $Mg^{2+}$, and $Cl^{-}$) is caused by anthropogenic factors such as irrigation water quality and unchecked fertilization; it is also strongly influenced by the local lithology. Both calcium and magnesium can come from the dissolution of calcium or magnesium sulphates. The transition from one dominant ratio to another can be done by dilution after mixing or precipitation of one of the ions. Regarding the origins of $Cl^{-}$, it may result from the soil's high levels of organic matter decomposing due to wastewater from "Doucen ville" [62]. Table 2 displays a statistical summary of the groundwater samples that were analyzed in relation to irrigation water standards.

**Table 2.** Descriptive outcomes of the groundwater samples with the standard limit for irrigation activities.

| Parameters | FAO * | Minimum | Maximum | Average | Standard Deviation |
|---|---|---|---|---|---|
| pH | 8.5 | 7.08 | 8.24 | 7.50 | 0.24 |
| TDS | 2000 | 1046 | 4650 | 2137 | 931 |
| EC | 3000 | 2091 | 9300 | 4274 | 1862 |
| $K^{+}$ | 2 | 2.00 | 50.00 | 16.89 | 13.20 |
| $Na^{+}$ | 919 | 50.00 | 340.00 | 167.11 | 89.98 |
| $Ca^{2+}$ | 400 | 176.00 | 561.00 | 353.48 | 110.30 |
| $Mg^{2+}$ | 60 | 75.00 | 423.00 | 155.44 | 84.31 |
| $SO_4^{2-}$ | 960 | 320.00 | 472.00 | 403.26 | 36.17 |
| $Cl^{-}$ | 1036 | 177.00 | 1808.00 | 621.67 | 384.37 |
| $HCO_3^{-}$ | 610 | 450.00 | 830.00 | 548.81 | 79.74 |
| $NO_3^{-}$ | 10 | 3.61 | 41.80 | 19.18 | 10.94 |

Note(s): FAO *: Food and Agricultural Organization [63].

According to the physicochemical parameters results (Table 2), the pH values varied from 7.08 to 8.24 with a mean value of 7.50, which represents a weakly alkaline environment [64]. The pH values of the collected samples were within the allowable limit for irrigation. The TDS values diverse from 1045.5 mg/L to 4950 mg/L with an average value of 2136.81 mg/L (Table 2). Moreover, the electrical conductivity (EC) values ranged from 9300 µS/cm to 2091 µs/cm, with an average value of 4273.62 µS/cm (Table 2). According to the results of EC values, the majority of our samples (74%) were unfit for irrigation purposes. Table 2 shows that the average $K^{+}$ content in our samples was 17.70 mg/L, with a range of 2–50 mg/L. This means that none of our groundwater samples are suitable for irrigation. Because of the high concentration of $K^{+}$, we can deduce that potash feldspars minerals have been weathered and that chemical fertilizers (NPK) have been dissolved [65]. Further, $Na^{+}$ concentrations extended from 50 to 340 mg/L, with an average of 168 mg/L, making all groundwater samples technically appropriate for irrigation (Table 2). The concentration of the $Ca^{+2}$ ion ranged from 176 to 561 mg/L, with a value of 353.48 mg/L serving as the average (Table 2). As shown by the $Ca^{+2}$ levels, the majority of the collected samples (78%) were acceptable for irrigation, while 22% were not. This discrepancy might be attributed to the impact of the dissolution of carbonate minerals from the gypsum deposits [66,67].

The concentration of $Mg^{2+}$ ions in the collected water samples extended from 75 to 423 mg/L, with an average value of 155.44 mg/L (Table 2), signifying that all groundwater samples were inappropriate for irrigation. The elevated concentration of $Mg^{2+}$ revealed leaching and ion exchange process of ferromagnesium minerals from the aquifer materials [68,69]. The $HCO_3^{-}$ concentrations were from 450 to 830 mg/L, with an average of 548.81 mg/L. According to $HCO_3^{-}$ values, the majority of samples (93%) were within the satisfactory limit for irrigation purposes consistent with the value guide of 610 mg/L [63]. According to [63], all of our groundwater samples were suitable for irrigation since their sulphate concentrations ranged from 320 to 472 mg/L, with an average of 403.29 mg/L (Table 2). Overall, the chloride concentrations in the groundwater samples that were taken diverse from 177 to 1808 mg/L, with an average of 621.66 mg/L (Table 2). Approximately 7% of the samples exceeded the required value related to irrigation, although the vast majority (93%) were under the permitted level for irrigation. Evaporitic formations, perhaps related to the local agro-food sector or urbanization via wastewater discharges [41], contributed to the elevated chloride concentrations found in the groundwater samples. Finally, the nitrate concentrations varied between 3.61 mg/L and 40.71 mg/L (average value of 20.48 mg/L), as indicated in Table 2.

More than two-thirds (67%) of the groundwater samples had nitrates values too high for irrigation, while 33% were completely unfit for the purpose.

The high concentration of $NO_3^-$ suggested anthropogenic activity due to excessive inorganic nitrogenous fertilizer application, home and industrial wastes, and intense irrigation [52,64,65,70].

### *3.2. Groundwater Facies and Source Identification*

#### 3.2.1. Groundwater Types

Geology, water-rock interaction, and groundwater flow pattern through the aquifer are important in the production and classification of water types, which are, in turn, explained by groundwater hydrochemical facies. To better understand the preponderance of major ions in the groundwater aquifer, a Piper diagram was developed to depict the geochemical attribution and hydrogeochemical properties of groundwater [71]. Rock-water interaction, ion exchange, weathering of soils, and salt-bearing sedimentary rock were the main geochemical controlling processes, as shown in Figure 3.

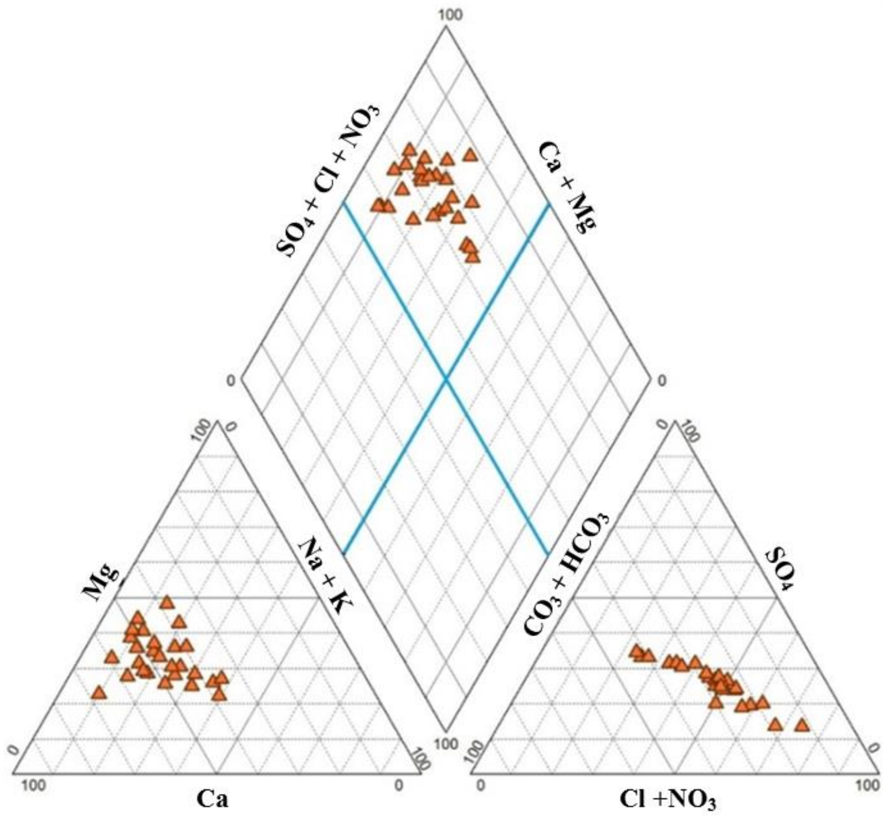


**Figure 3.** Groundwater facies according to Piper diagram.

#### 3.2.2. Processes Influencing Groundwater Chemistry

The diagram of Gibbs can help in identifying the variables that affect the hydrochemistry of groundwater [72]. It classified the water into three types such as precipitation dominance, rock dominance, and evaporation dominance [73,74]. As shown in Figure 4, water-rock interactions appear to be the predominant natural process governing water chemistry, as evidenced by the fact that groundwater samples cluster in the rock weathering dominating field and the evaporation zone dominance. Furthermore, the ratios of $Na^+/(Na^+ + Ca^{2+})$ were from 0.31 to 0.53; an average of 0.31 was recorded, which showed a robust cation exchange in the organization [47,75] according to Equations (5) and (6):

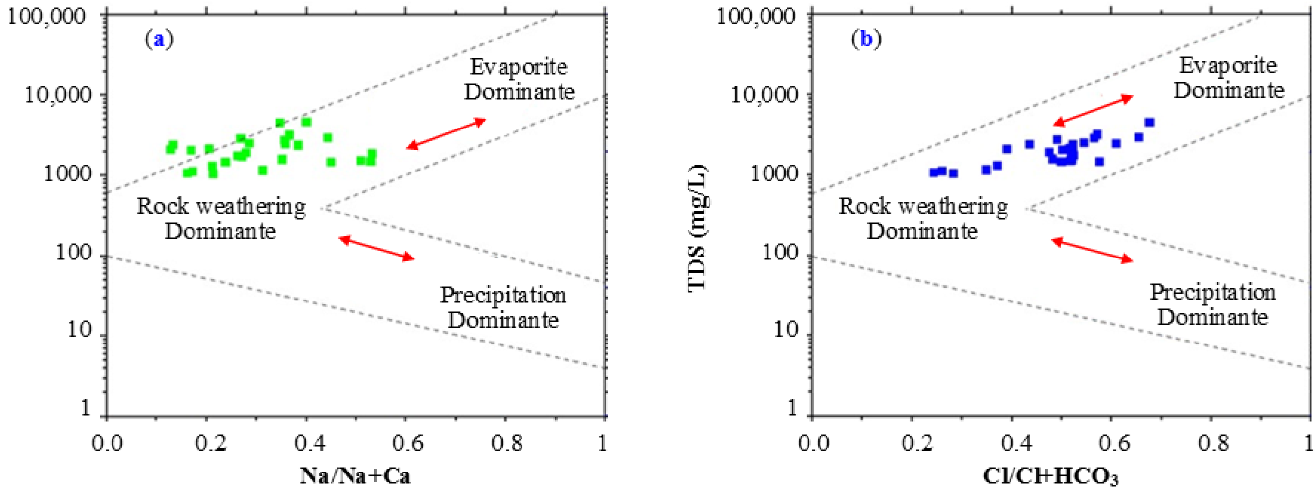


**Figure 4.** Geochemical controlling mechanisms according to Gibbs diagram: (**a**) TDS vs. Na/Na+Ca, and (**b**) TDS vs. Cl/Cl+$HCO_3$.

Ion exchange:

$$2NaX + Ca^{2+} \rightarrow 2Na^+ + CaX^2 \tag{5}$$

Reverse Ion exchange:

$$CaX^2 + 2Na^+ \rightarrow Ca^{2+} + 2NaX \tag{6}$$

The scatter plot $HCO_3$/Na versus Ca/Na revealed a high influence on the weathering process (Figure 5a). Generally, the dissolution of calcite minerals and dolomite was responsible for high $Ca^{2+}$ and $Mg^{2+}$ along with $HCO_3^-$ ions in groundwater [76,77]. Moreover, the scatter plot between Mg/Na and Ca/Na demonstrated that the main mechanism and factor contributing to the presence of magnesium in groundwater is silicate weathering (Figure 5b). Nonetheless, the $Ca^{2+} + Mg^{2+}$ vs. $HCO_3^- + SO_4^{2-}$ relations of most groundwater samples (Figure 5c) revealed the non-dominancy of carbonate weathering in the study area. The plotting of $Ca^{2+} + Mg^{2+}$ versus $HCO_3^-$ (Figure 5d) indicated an excess of $HCO_3^-$ due to rock weathering and the ion exchange process, which was a prime mechanism to release the $HCO_3^-$ into the groundwater [78]. Consequently, $Na^+$: $Cl^-$ ratios in the majority of samples were lower than unity (Figure 5e). According to Figure 5e, the ratio of $Na^+/Cl^-$ was 0.28, indicating another chloride source [79]. Finally, chloro-alkaline indices (CAI) were applied to examine the cation exchange process and geochemical controlling mechanisms on the groundwater chemistry. The CAI values such as CAI 1 and CAI 2 showed positive values (Figure 5f), which indicates high cation exchange tendency between the $Ca^{2+}$ and $Mg^{2+}$ in the surrounding rock and $Na^+$ and $K^+$ in the groundwater [75,80,81].

### *3.3. Analysis of Multivariate Statistics*

#### 3.3.1. Cluster Analysis

Concerning the similarity of the groundwater samples, a combination of Ward's linkage technique and Euclidean distance were used. In Figure 6, the Dendrogram was displayed to classify the different physicochemical variables in the obtained groundwater samples. In order to roughly match normally distributed data, all variables were log-transformed. Standard scores (z-scores) were calculated and applied to each variable [82].

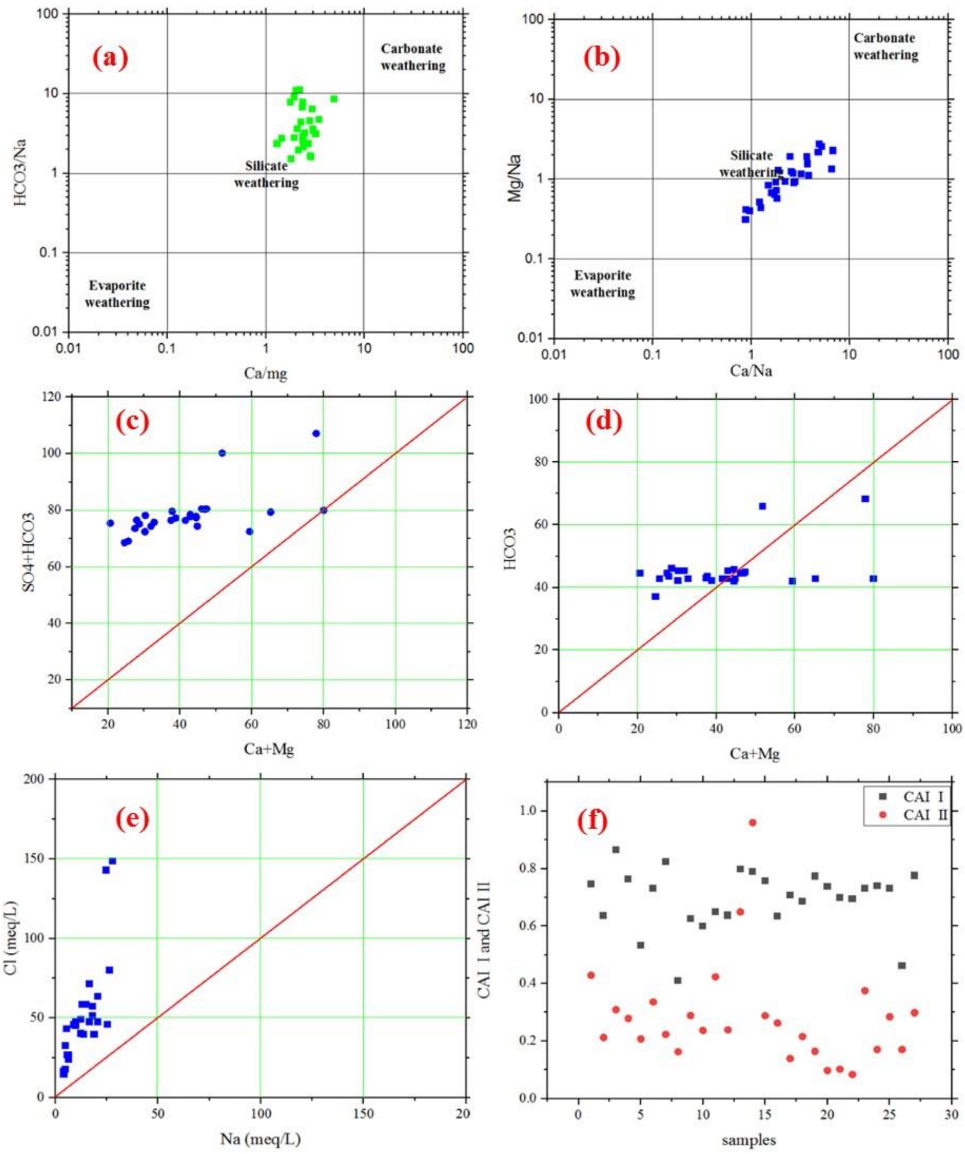


**Figure 5.** Major cations and anions in the research region and their stoichiometric relationships: (**a**) [$HCO_3^-/Na^+$] vs. [$Ca^{2+}/Mg^{2+}$], (**b**) [$Ca^{2+}/Na^+$] vs. [$Mg^{2+}/Na^+$], (**c**) [$Ca^{2+}$ + $Mg^{2+}$] vs. [$SO_4^{2-}$ + $HCO_3^-$], (**d**) [$Ca^{2+}$ + $Mg^{2+}$] vs. [$HCO_3^-$], (**e**) [$Na^+$] vs. [$Cl^-$], and (**f**) [CAI 1, CAI 2].

The Dendrogram of the ten physicochemical parameters ($Mg^{2+}$, $Ca^{2+}$, $K^+$, $Na^+$, $Cl^-$, $HCO_3^-$, $NO_3^-$, $SO_4^{2-}$, EC and TDS) had been divided into three main groups (Figure 6). The obtained results revealed that TDS and EC were the major distinction parameters. The first group (G1) revealed a close association between the carbonate's parameters $HCO_3^-$, $SO_4^{2-}$, $Mg^{2+}$, and $Ca^{2+}$, due to the major predominance of $Mg^{2+}$, $Ca^{2+}$ in the chemical composition of our groundwaters, such as sulphates or anhydride and calcium sulphates. The second group (G2) revealed a close association between the evaporate parameters. For example, $Na^+$, $K^+$, $Cl^-$, EC, and TDS, indicate the main participation of chlorides and salts in the electrical conductivity with the dominance of $Cl^-$ in the chemical composition of groundwater in the study region. Both G1 and G2 demonstrated that the lithological component dominated the mineralization of the Plio-Quaternary aquifer's waters in Doucen. Finally, the third group (G3) showed a close association between $Mg^{2+}$ and $Ca^{2+}$, indicating the probable same origin of these two elements. G3 showed the dissociation of nitrates from other chemical elements present in groundwater, which indicates an anthropogenic source.

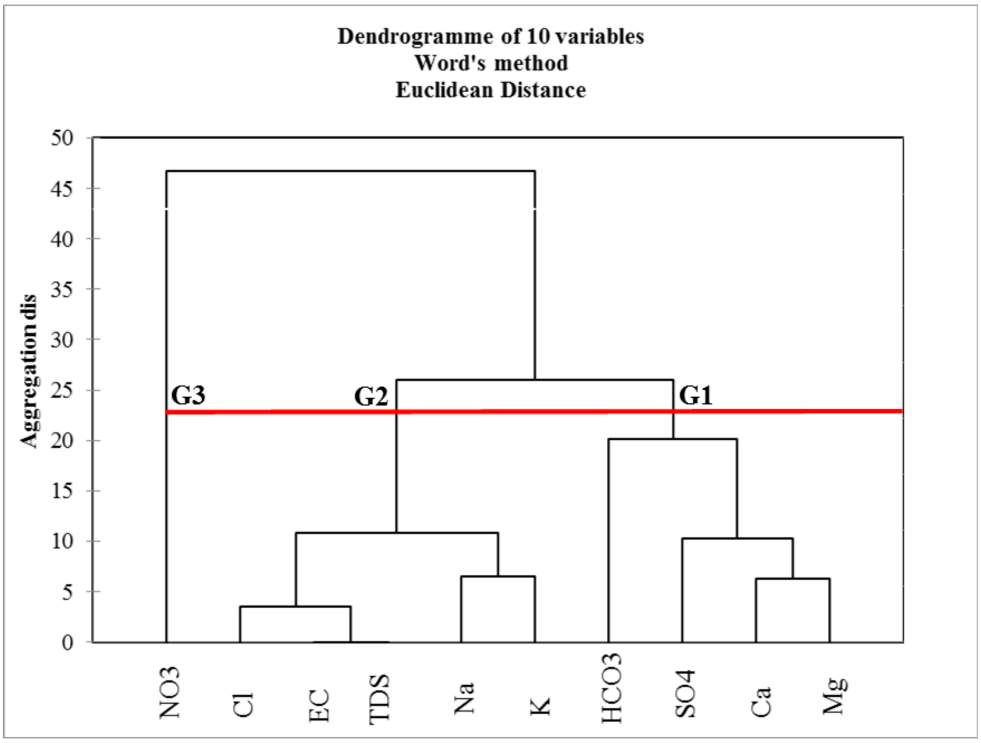


**Figure 6.** Cluster dendrogram for variables: G1 (group 1), G2 (group 2), G3 (group 3) and the groups could be distinguished in terms of their hydrochemical variable at the red line.

3.3.2. Principal Component Analysis (PCA)

Three factors (F) were retained from the PCA analysis with an Eigen value of more than one. F1 explained 59.86% of the dataset variability, while F2 and F3 explained, respectively, 11.35% and 10.35% (Figure 7). The value of the variable loading is presented in Table 3. The value close to $\pm 1$ revealed a high correlation between the factor and the variables. These loadings are further categorized into three categories, such as strong (>$\pm 0.75$), moderate ($\pm 0.75$ to $\pm 0.50$), and weak ($\pm 0.50$ to $\pm 0.30$), as reported by Hinge et al. [44,74]. F1 has a robust positive relationship with TDS, EC, $Cl^-$, $Ca^{3+}$, $Mg^{2+}$, $K^+$, and $SO_4{}^{2-}$. The source of $SO_4{}^{2-}$ may be oxidation of $SO_4{}^{2-}$ coming from fertilizer and sulfur compounds. The $Ca^{2+}$, $Mg^{2+}$, and $K^+$ could be due to anthropogenic sources, such as irrigation water quality, domestic waste, and uncontrolled fertilization. The presence of chloride could be due to weathering of soils and salt-bearing formation. F2 was moderately correlated with $Na^+$, while F3 was highly correlated with $NO_3{}^-$ and moderate correlation with $HCO_3{}^-$, which indicates alkaline water passing through rocks and soil. These results shed light on the methods through which human activities, rock weathering, and the ion exchange process affect groundwater quality.

### *3.4. Irrigation Water Quality Indices*

Based on the parameters' standard value intervals, we classified the quality of the irrigation water in our study area using the IWQI, SAR, KI, MH, Na%, and PI (Table 4).

3.4.1. Irrigation Water Quality Index

IWQI involves the usage of either individual chemical indices [81,83–85] or several associated indices [47,86,87]. Although evaluating groundwater for irrigation based on individual characteristics is useful, the combined indices give decision-makers more insightful information.

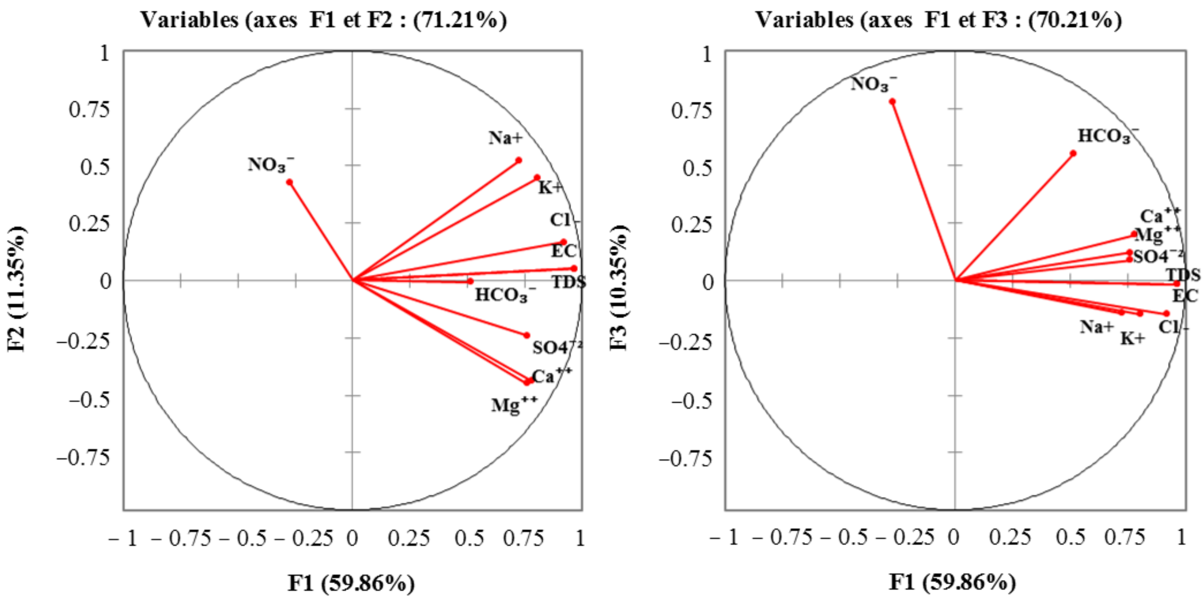


**Figure 7.** Plots of PCA scores for F2 vs. F1 (**a**) and F3 vs. F1 (**b**).

**Table 3.** Correlation between the different physicochemical parameters and factors.

| Parameter | F1 | F2 | F3 |
|---|---|---|---|
| EC | 0.965 | 0.051 | −0.016 |
| TDS | 0.965 | 0.051 | −0.016 |
| $Ca^{2+}$ | 0.781 | −0.438 | 0.200 |
| $Mg^{2+}$ | 0.761 | −0.448 | 0.121 |
| $HCO_3^-$ | 0.514 | −0.007 | 0.551 |
| $Cl^-$ | 0.920 | 0.166 | −0.148 |
| $Na^+$ | 0.724 | 0.522 | −0.141 |
| $K^+$ | 0.805 | 0.444 | −0.147 |
| $SO_4^{2-}$ | 0.761 | −0.241 | 0.089 |
| $NO_3^-$ | −0.274 | 0.427 | 0.778 |

F1 (factor 1), F2 (factor 2), F3 (factor 3).

**Table 4.** Statistical analysis and classes of IWQIs.

| Criteria | Min | Max | Mean | Range | Class | Number of Samples (%) |
|---|---|---|---|---|---|---|
| IWQI | 19.01 | 73.61 | 47.17 | 85–100 | No restriction | 0 (0.0%) |
| | | | | 70–85 | Low restriction | 0 (0.0%) |
| | | | | 55–70 | Moderate restriction | 9 (33.33%) |
| | | | | 40–55 | High restriction | 9 (33.33%) |
| | | | | 0–40 | Severe restriction | 9 (33.33%) |
| SAR | 0.63 | 4.10 | 1.88 | <10 | Excellent | 27 (100%) |
| | | | | 10–18 | Good | 0.00 |
| | | | | 19–26 | Fair Poor | 0.00 |
| | | | | >26 | Unsuitable | 0.00 |
| KI | 0.08 | 0.62 | 0.25 | <1 | Suitable | 27 (100%) |
| | | | | >1 | Unsuitable | 0.00 |
| Na% | 7.88 | 39.31 | 19.96 | <20% | Excellent | 16 (59.26%) |
| | | | | 21–40% | Good | 11 (40.74%) |
| | | | | 41–60% | Permissible | 0.00 |
| | | | | 61–80% | Doubtful | 0.00 |
| | | | | >80% | Unsuitable | 0.00 |
| MH | 25.38 | 56.22 | 41.18 | <50% | Suitable | 25 (92.59%) |
| | | | | >50% | Unsuitable | 2 (7.41%) |
| PI | 13.95 | 46.68 | 27.87 | >75% | Suitable | 0.00 |
| | | | | 25–75% | Moderate | 15 (55.55%) |
| | | | | <25% | Unsuitable | 12 (44.44%) |

In this study, five hazard parameters have been used: SAR, EC, Cl, Na, and $HCO_3$, to judge the groundwater's viability for irrigation in agriculture [47]. The resulting IWQI value varies from 19.01 to 73.61, with an average value of 47.17. The IWQI suitability categorization of groundwater samples falls into three categories (moderate, high, and severe restriction) with an equal 33.33% (Table 4). Based on physicochemical parameters, the overall index map shows the water's appropriateness for irrigation (Figure 8a). A map can be used to estimate groundwater validation for irrigation. According to IWQI values, the central region of our region has documented water quality degradation brought on by anthropogenic activities and geogenic sources (rock weathering and the ion exchange process).

### 3.4.2. Sodium Adsorption Ratio

The ability of the soil structure in the aquifer is shown by the sodium adsorption ratio. SAR is also employed in irrigation water to remove $Ca^{2+}$ and $Mg^{2+}$ ions and acquire $Na^+$ ions from groundwater at ion-exchangeable sites, potentially causing soil particle dispersion and a decrease in infiltration capacity [88,89]. Whilst significant salinity of water can benefit the structure of the soil by improving the infiltration rate, which causes more water stress in plants. Table 4 shows that the calculated percent of SAR in groundwater samples varied from 0.63% to 4.1% (mean of 1.88%). According to sodium adsorption (SAR), four classes were created to identify the irrigation water [48], unsuitable (>26%), fair poor (19–26%), good (10–18%), and excellent (<10%). The value of SAR indicated that all of the study site's water samples belong to the excellent category, which indicates its suitability for irrigation (Figure 8b). These results showed that irrigated water had no impact on crop output or soil infiltration.

### 3.4.3. Kelly Index

Groundwater suitability for irrigation was determined using the KI method, and the results indicated an overabundance of sodium ions in the water [90]. The KI value was diverse from 0.08 to 0.62, with a mean value of 0.25. With regards to the KI outcomes, 100% of the groundwater samples were deemed irrigation-ready (Table 4 and Figure 8c). If the KI value is greater than one (KI > 1), there is too much sodium present, whereas a number lower than one (KI < 1) denotes irrigation-ready water [91,92].

### 3.4.4. Sodium Percentage

Since $Na^+$ concentrations have a negative effect on soil permeability, Na% can be utilized to define whether or not water is appropriate for irrigation purposes [93]. Clay minerals remove $Mg^{2+}$ ions and $Ca^{2+}$ from irrigation water by absorbing excess $Na^+$. $Na^+$ in water is exchanged for $Ca^{2+}$ and $Mg^{2+}$ in soil, reducing permittivity and, therefore, soil penetration. Sodium concentration ranged from 7.88% to 39.31%, with a mean of 19.95% across all samples (Table 4). There are five categories for the quality of irrigation water depending on the Na% value [94]: excellent (20%), acceptable (20–40%), allowed (40–60%), dubious (60–80%), and inappropriate (>80%). About 59.26% of the samples are in the excellent class, and these are positioned in the north, south east, and south west of the tested area. Nonetheless, about 40.74% of the samples are in the ideal category for irrigation and are located in the geographic center of the region (Figure 8d).

### 3.4.5. Magnesium Hazards

MH, defined as the ratio of magnesium to calcium in the water, was estimated using the above-mentioned equation (Table 1). As shown in the MH value, there are two main categories of groundwater utilization in irrigation. If the MH value is below 50%, the water is considered appropriate, whereas if it is above 50%, it is deemed unsuitable [95]. The rate at which soil absorbs water from irrigation may be affected by the adsorption of clay minerals to $Mg^{2+}$ ions in water if the concentration of Mg ions is larger than that of calcium ions [89]. The groundwater samples showed the MH value varied from 25.38 to 56.22, with a mean value of 41.17. With an MH value of less than 50, groundwater was appropriate for irrigation in 25 samples, while with an MH value of more than 50, it was not (Figure 8e). These inappropriate samples are situated in the research area's northern region.

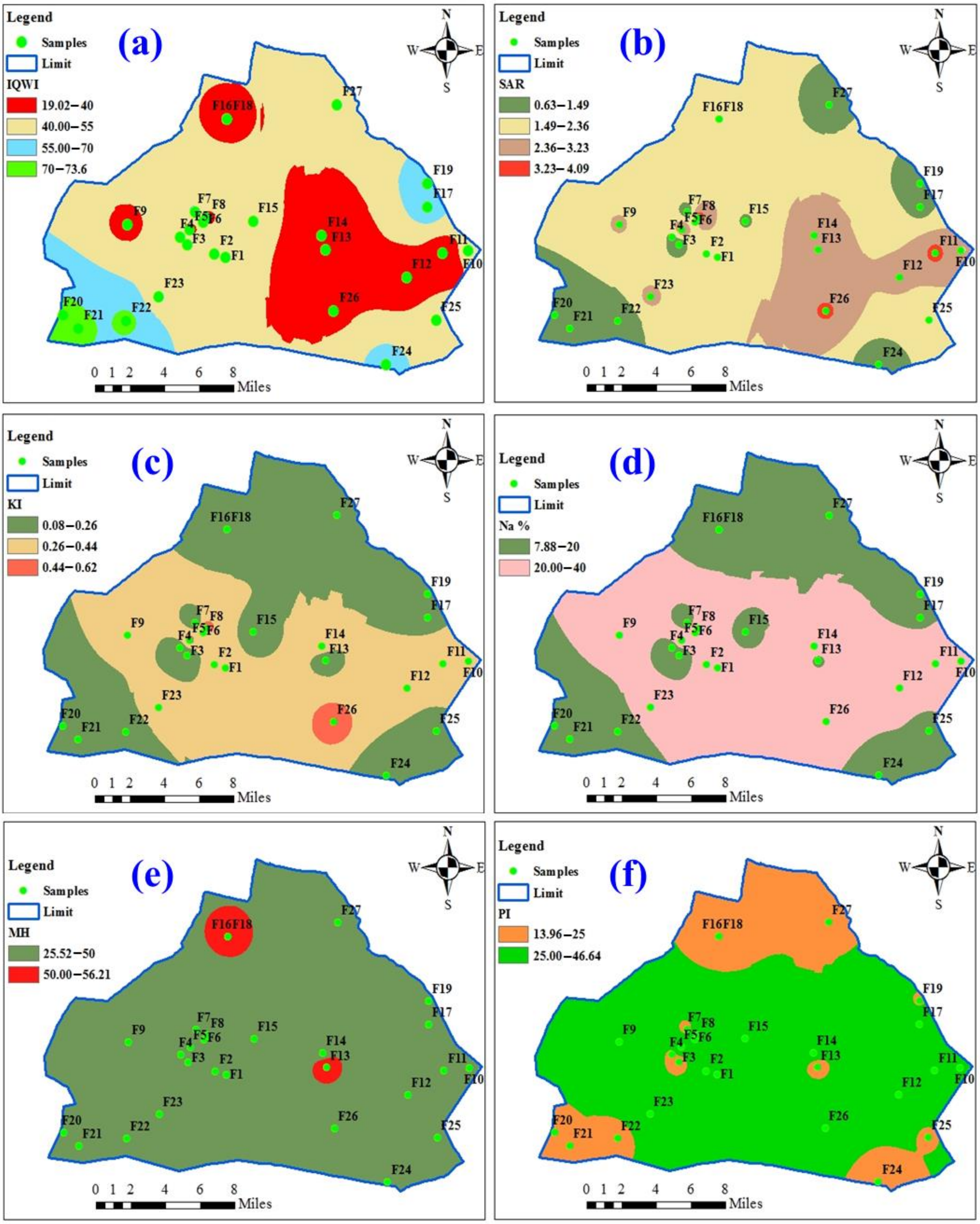


**Figure 8.** The spatial variation map of the Doucen plain: Irrigation water quality indices (IWQIs). (**a**) IQWI, (**b**) SAR, (**c**) KI, (**d**) Na%, (**e**) MH, (**f**) PI.

### 3.4.6. Permeability Index

Since irrigation water consumption has a lasting effect on soil permeability, the PI serves as a vital gauge of irrigation water quality; it is regulated by bicarbonate, calcium, magnesium, and sodium ions found in the soil. To decide whether or not groundwater is suitable for irrigation [96], the parameter PI was used with the following cutoffs: unsuitable (PI = 25), good (PI = 25–75), and excellent (PI > 75). The PI value for our samples was reported to range from 13.95 to 46.68, with an average value of 27.86. Approximately 55.55% of the water samples were found in the moderate class, and the rest (44.44%) were unsuitable for irrigation; these samples were located in the north, south east, and south west of our area (Figure 8f).

## 4. IWQIs Prediction Using GBR and ANN

The high-level variables were filtered using the studied parameters, as shown in Table 5 and Figure 9, using the GBR and ANN models. These characteristics contributed to the identification of IWQI, SAR, KI, Na%, MH, and PI. The training and testing results (accuracy and RMSE) for forecasting the investigated parameters using the GBR and ANN models are publicized in Table 5 and Figure 9. The unused reserved values of GBR and ANN models were compared to the expected values. Results from the present study examination and comparison of multivariate methods show that this approach significantly improves predictability. Relying on independent validation to assess the accuracy of a regression model is preferable since validation data are not incorporated into the model construction practice. In this work, to forecast each output, the ANN model has surpassed the GBR model. The findings showed that the ANN-2F had the highest correlation between IWQI and the exceptional features, making it the most accurate prediction model. This model has roughly two qualities that are critical for IWQI prediction. The $R^2$ and RMSE values for the training and validation sets were 0.973, 2.492, and 0.958, 2.175, respectively. When measuring SAR, the ANN-3F model had the best outcomes. In the training set, the $R^2$ value was 0.999 (RMSE = 0.003), and in the testing phase, it was 0.999 (RMSE = 0.006). The most accurate model (ANN-3F) for determining KI had RMSE values for the training and testing sets of 0.002 and 0.004, respectively, and $R^2$ values of 0.999, and 0.999, respectively. Na% predictions were most accurate with the ANN-2F model. Regarding the training and test sets, the model achieved an $R^2$ of 1.0 (RMSE = $2.306 \times 10^{-7}$) and 1.0 (RMSE = $4.169 \times 10^{-7}$). The ANN-2F model accurately forecasted the MH. $R^2$ scores for the training and testing sets were 0.999 (RMSE = 0.005 and 0.036, respectively). In terms of predicting the PI, the ANN-4F model outscored other models. With $R^2$ values of 0.999 for the training set and 0.999 for the testing set (RMSE = 0.003 and 0.106, respectively), the model completed well. According to [97], who assert that the performance exceeded expectations, several techniques, including filtering high-level characteristics and changing model hyperparameters, were necessary to update regression approaches for correct prediction. In four main areas, deep learning algorithms exceed expectations: selecting the most relevant feature from an image's color space, integrating image data with information about plants' surroundings, augmenting data, and merging separate trained deep networks [98].

**Table 5.** The outcomes of GBR and ANN models based on optimal features.

| Variable | Model | Optimal Features (F) | Hyper-Parameters | Training | | Validation | |
|---|---|---|---|---|---|---|---|
| | | | | $R^2$ | RMSE | $R^2$ | RMSE |
| IWQI | GBR | EC, $Na^+$, $Cl^-$ | (Ns = 25, Mf = log2) | 0.991 | 1.481 | 0.951 | 2.562 |
| | ANN | $Cl^-$, $Na^+$ | ($h_1$ = 18, $h_2$ = 9, fun = relu) | 0.973 | 2.492 | 0.958 | 2.175 |
| SAR | GBR | $Mg^{2+}$, $Na^+$ | (Ns = 25, Mf = log2) | 0.983 | 0.128 | 0.841 | 0.294 |
| | ANN | $Ca^{2+}$, $Mg^{2+}$, $Na^+$ | ($h_1$ = 9, $h_2$ = 12, fun = logistic) | 0.999 | 0.003 | 0.999 | 0.006 |
| KI | GBR | $Mg^{2+}$, $Na^+$ | (Ns = 25, Mf = log2) | 0.981 | 0.020 | 0.763 | 0.054 |
| | ANN | $Mg^{2+}$, $Na^+$, $Ca^{2+}$ | ($h_1$ = 6, $h_2$ = 15, fun = tanh) | 0.999 | 0.002 | 0.999 | 0.004 |
| Na% | GBR | $Mg^{2+}$, $Ca^{2+}$, $Na^+$ | (Ns = 25, Mf = auto) | 0.990 | 0.909 | 0.783 | 3.186 |
| | ANN | $Ca^{2+}$, $Na^+$ | ($h_1$ = 3, $h_2$ = 18, fun = identity) | 1.0 | $2.306 \times 10^{-7}$ | 1.0 | $4.169 \times 10^{-7}$ |
| MH | GBR | $Ca^{2+}$, $Mg^{2+}$ | (Ns = 25, Mf = auto) | 0.969 | 1.125 | 0.557 | 2.946 |
| | ANN | $Ca^{2+}$, $Mg^{2+}$ | ($h_1$ = 9, $h_2$ = 9, fun = logistic) | 0.999 | 0.005 | 0.999 | 0.036 |
| PI | GBR | $Na^+$, $Mg^{2+}$ | (Ns = 25, Mf = auto) | 0.984 | 1.093 | 0.577 | 4.147 |
| | ANN | $HCO_3^-$, $Mg^{2+}$, $Ca^{2+}$, $Na^+$ | ($h_1$ = 18, $h_2$ = 15, fun = logistic) | 0.999 | 0.003 | 0.999 | 0.106 |

Note(s): where Ns is the number of boosting stages to perform, Mf is the number of features to consider when looking for the best split, $h_1$ and $h_2$ are amount of neurons in the two hidden layers, and fun is the activation function.

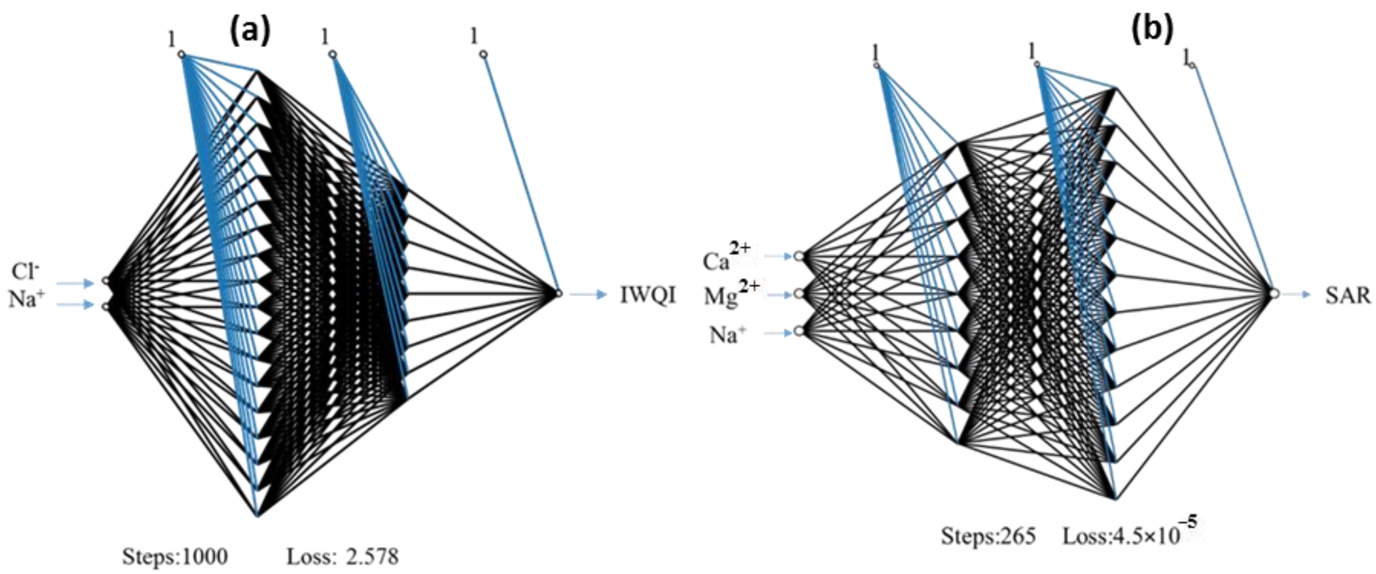


**Figure 9.** *Cont.*

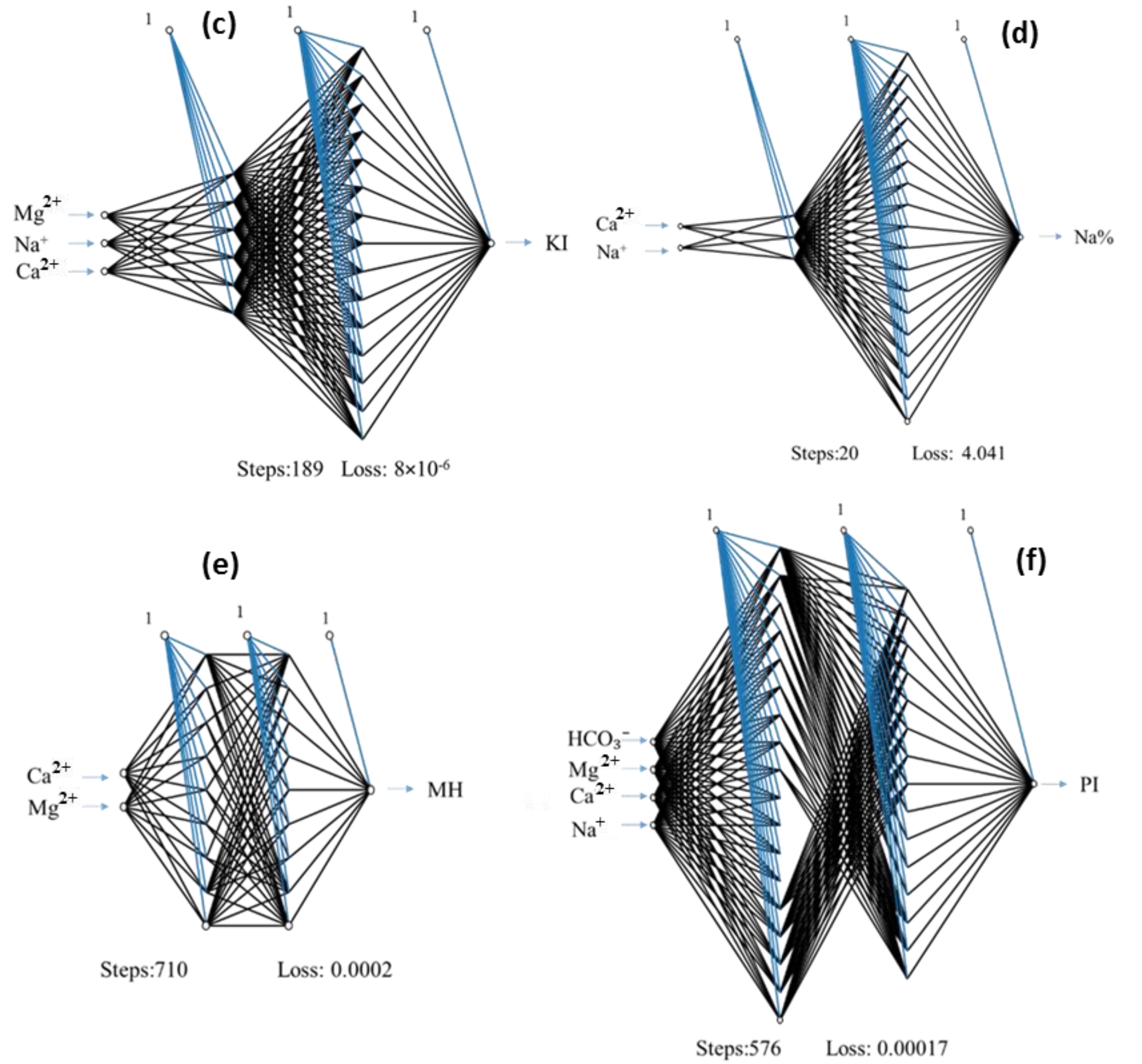


**Figure 9.** The ideal ANN architecture for detecting spatial groundwater quality variations: (**a**) IWQI, (**b**) SAR, (**c**) KI, (**d**) Na%, (**e**) MH, and (**f**) PI.

## 5. Conclusions

In this study, IWQIs, multivariate statistical analyses, GBR, and ANN models, backed by GIS techniques, were applied to determine groundwater quality for irrigation in the Doucen Plain, Northeastern Ouled Djelal, Algeria. According to the physicochemical results, groundwater in the study area revealed ion sequences of $Ca^{2+} > Mg^{2+} > Na^{+} > K^{+}$, and $Cl^{-} > SO_4^{2-} > HCO_3^{-} > NO_3^{-}$, which indicates Ca-Cl water type due to the dominance of sandstone, limestone and clay minerals under the influence of anthropogenic activities, rock weathering, ion dissolution, and exchange processes. The IWQI values revealed that 33% of our samples were severely restricted for irrigation, while 67% were diverse from moderate to high constraints for irrigation. In addition, SAR, KI, Na%, MH, and PI% showed that 100.0%, 100.0%, 59.0%, 92.0%, and 44.0% of groundwater samples were classified as excellent, suitable, excellent, suitable, and suitable, respectively. The

ANN model has surpassed the GBR model. The findings showed that the ANN-2F had the highest correlation between IWQI and the exceptional features, making it the most accurate prediction model. For example, the most accurate model (ANN-3F) for determining KI had RMSE values for the training and testing sets of 0.002 and 0.004, respectively, with $R^2$ values of 0.999 and 0.999. Accordingly, an effective and practical strategy for assessing the quality of groundwater and its development is the use of physicochemical parameters and water quality indices supported by GIS techniques, multivariate modeling, and machine learning.

**Supplementary Materials:** The following supporting information can be downloaded at: https://www.mdpi.com/article/10.3390/w15020289/s1, Figure S1. Summary of the geological units of the Biskra region.

**Author Contributions:** Conceptualization, A.G., M.G. and S.E.; fieldwork, A.G., H.A.A., S.B. and G.H.; methodology, M.G., S.E., S.H. and H.I.; software, M.G., S.E., O.E. and H.I.; validation, S.E., O.E., M.H.E. and M.G.; formal analysis, H.A.A., S.B., G.H. and A.A.; investigation, A.G., S.B., G.H. and S.H.; resources, A.G. and M.G.; data curation, A.G.; writing original draft preparation, A.G., H.A.A., M.G. and S.E.; writing—review and editing, A.G., H.A.A., M.G. and S.E.; supervision, M.G. and S.E.; project administration, A.G. All authors have read and agreed to the published version of the manuscript.

**Funding:** This research received no external funding.

**Data Availability Statement:** All data are provided as tables and figures.

**Acknowledgments:** Considerable appreciation is addressed to the DGRSDT and the MESRS for their valuable support.

**Conflicts of Interest:** The authors declare that they have no known competing financial interests or personal relationships that could have appeared to influence the work reported in this paper.

## References

1. Wada, Y.; van Beek, L.P.H.; van Kempen, C.M.; Reckman, J.W.T.M.; Vasak, S.; Bierkens, M.F.P. Global Depletion of Groundwater Resources: Global groundwater depletion. *Geophys. Res. Lett.* **2010**, *37*, L20402. [CrossRef]
2. Naz, A.; Mishra, B.K.; Gupta, S.K. Human Health Risk Assessment of Chromium in Drinking Water: A Case Study of Sukinda Chromite Mine, Odisha, India. *Expo Health* **2016**, *8*, 253–264. [CrossRef]
3. Gaagai, A. Etude de l'Evolution de la Qualité des Eaux du Barrage de Babar (Sud-Est Algérien) et l'Impact de la Rupture de la Digue sur l'Environnement. Ph.D. Thesis, University of Batna 2, Batna, Algeria, 2017. [CrossRef]
4. Athamena, A.; Menani, M.R. Nitrogen Flux and Hydrochemical Characteristics of the Calcareous Aquifer of the Zana Plain, North East of Algeria. *Arab. J. Geosci.* **2018**, *11*, 356. [CrossRef]
5. Koull, N.; Helimi, S.; Mihoub, A.; Mokhtari, S.; Kherraze, M.E.; Aouissi, H.A.; Koull, N.; Helimi, S.; Mihoub, A.; Mokhtari, S.; et al. Integración de SIG y Análisis Jerárquico Multi-Criterio Para Analizar La Idoneidad de La Tierra Para Los Cereales En La Zona Árida de Argelia. *Int. J. Agric. Nat. Resour.* **2022**, *49*, 36–50. [CrossRef]
6. Belalite, H.; Menani, M.R.; Athamena, A. Calculation of Water Needs of the Main Crops and Water Resources Available in a Semi-Arid Climate, Case of Zana-Gadaïne Plain, Northeastern Algeria. *Alger. J. Environ. Sci. Technol.* **2022**, *8*, 2477–2488.
7. Egbueri, J.C.; Ezugwu, C.K.; Unigwe, C.O.; Onwuka, O.S.; Onyemesili, O.C.; Mgbenu, C.N. Multidimensional Analysis of the Contamination Status, Corrosivity and Hydrogeochemistry of Groundwater from Parts of the Anambra Basin, Nigeria. *Anal. Lett.* **2021**, *54*, 2126–2156. [CrossRef]
8. Noori, R.; Ghahremanzadeh, H.; Kløve, B.; Adamowski, J.F.; Baghvand, A. Modified-DRASTIC, modified-SINTACS and SI methods for groundwater vulnerability assessment in the southern Tehran aquifer. *J. Environ. Sci. Health* **2019**, *54*, 89–100. [CrossRef]
9. Noori, R.; Maghrebi, M.; Mirchi, A.; Tang, Q.; Bhattarai, R.; Sadegh, M.; Nouryh, M.; Haghighia, A.T.; Kløvea, B.; Madani, K. Anthropogenic depletion of Iran's aquifers. *Proc. Natl. Acad. Sci. USA* **2021**, *118*, e2024221118. [CrossRef]
10. Maghrebi, M.; Noori, R.; Partani, S.; Araghi, A.; Barati, R.; Farnoush, H.; Haghighi, A.T. Iran's groundwater hydrochemistry. *Earth Space Sci.* **2021**, *8*, e2021EA001793. [CrossRef]
11. Ghodbane, M.; Benaabidate, L.; Boudoukha, A.; Gaagai, A.; Adjissi, O.; Chaib, W.; Aouissi, H.A. Analysis of groundwater quality in the lower Soummam Valley, North-East of Algeria. *J. Water Land Dev.* **2022**, *54*, 1–12. [CrossRef]
12. Chorfi, A.; Hafid, H.; Baaloudj, A.; Rizi, H.; Aouissi, H.A.; Chaib, S.; Ababsa, M.; Allaoua, N.; Houhamdi, M. Characterization and Diversity of Macroin-Vertebrates in Groundwater in the Region of Souk-Ahras (North-East of Algeria). *Ekológia* **2022**, *41*, 219–227. [CrossRef]

13. Şener, Ş.; Şener, E.; Davraz, A. Evaluation of Water Quality Using Water Quality Index (WQI) Method and GIS in Aksu River (SW-Turkey). *Sci. Total Environ.* **2017**, *584–585*, 131–144. [CrossRef]
14. Elsayed, S.; Hussein, H.; Moghanm, F.S.; Khedher, K.M.; Eid, E.M.; Gad, M. Application of Irrigation Water Quality Indices and Multivariate Statistical Techniques for Surface Water Quality Assessments in the Northern Nile Delta, Egypt. *Water* **2020**, *12*, 3300. [CrossRef]
15. El Osta, M.; Masoud, M.; Alqarawy, A.; Elsayed, S.; Gad, M. Groundwater Suitability for Drinking and Irrigation Using Water Quality Indices and Multivariate Modeling in Makkah Al-Mukarramah Province, Saudi Arabia. *Water* **2022**, *14*, 483. [CrossRef]
16. Masoud, M.; El Osta, M.; Alqarawy, A.; Elsayed, S.; Gad, M. Evaluation of Groundwater Quality for Agricultural under Different Conditions Using Water Quality Indices, Partial Least Squares Regression Models, and GIS Approaches. *Appl. Water Sci.* **2022**, *12*, 244. [CrossRef]
17. Gad, M.; El-Hendawy, S.; Al-Suhaibani, N.; Tahir, M.U.; Mubushar, M.; Elsayed, S. Combining Hydrogeochemical Characterization and a Hyperspectral Reflectance Tool for Assessing Quality and Suitability of Two Groundwater Resources for Irrigation in Egypt. *Water* **2020**, *12*, 2169. [CrossRef]
18. Aouissi, H.A.; Ababsa, M.; Gaagai, A.; Bouslama, Z.; Farhi, Y.; Chenchouni, H. Does Melanin-Based Plumage Coloration Reflect Health Status of Free-Living Birds in Urban Environments? *Avian Res.* **2021**, *12*, 45. [CrossRef]
19. Gad, M.; Abou El-Safa, M.M.; Farouk, M.; Hussein, H.; Alnemari, A.M.; Elsayed, S.; Khalifa, M.M.; Moghanm, F.S.; Eid, E.M.; Saleh, A.H. Integration of Water Quality Indices and Multivariate Modeling for Assessing Surface Water Quality in Qaroun Lake, Egypt. *Water* **2021**, *13*, 2258. [CrossRef]
20. Nas, B.; Berktay, A. Groundwater Quality Mapping in Urban Groundwater Using GIS. *Environ. Monit. Assess.* **2010**, *160*, 215–227. [CrossRef]
21. Gilbert, C.; Browell, J.; McMillan, D. Leveraging Turbine-Level Data for Improved Probabilistic Wind Power Forecasting. *IEEE Trans. Sustain. Energy* **2020**, *11*, 1152–1160. [CrossRef]
22. Nayak, A.; Matta, G.; Uniyal, D.P. Hydrochemical Characterization of Groundwater Quality Using Chemometric Analysis and Water Quality Indices in the Foothills of Himalayas. *Environ. Dev. Sustain.* **2022**, 1–32. [CrossRef] [PubMed]
23. Vincevica-Gaile, Z.; Sachpazidou, V.; Bisters, V.; Klavins, M.; Anne, O.; Grinfelde, I.; Hanc, E.; Hogland, W.; Ibrahim, M.A.; Jani, Y.; et al. Applying Macroalgal Biomass as an Energy Source: Utility of the Baltic Sea Beach Wrack for Thermochemical Conversion. *Sustainability* **2022**, *14*, 13712. [CrossRef]
24. Yotova, G.; Varbanov, M.; Tcherkezova, E.; Tsakovski, S. Water quality assessment of a river catchment by the composite water quality index and self-organizing maps. *Ecol. Indic.* **2021**, *120*, 106872. [CrossRef]
25. Kebaili, F.K.; Baziz-Berkani, A.; Aouissi, H.A.; Mihai, F.-C.; Houda, M.; Ababsa, M.; Azab, M.; Petrisor, A.-I.; Fürst, C. Characterization and Planning of Household Waste Management: A Case Study from the MENA Region. *Sustainability* **2022**, *14*, 5461. [CrossRef]
26. Varbanov, M.; Gartsiyanova, K.; Tcherkezova, E.; Kitev, A.; Genchev, S. Analysis of the quality of river water in Sofia city district, Bulgaria. *J. Phys. Conf. Ser.* **2021**, *1960*, 012019. [CrossRef]
27. He, S.; Wu, J. Relationships of Groundwater Quality and Associated Health Risks with Land Use/Land Cover Patterns: A Case Study in a Loess Area, Northwest China. *Hum. Ecol. Risk Assess. Int. J.* **2019**, *25*, 354–373. [CrossRef]
28. Gad, M.; Saleh, A.H.; Hussein, H.; Farouk, M.; Elsayed, S. Appraisal of Surface Water Quality of Nile River Using Water Quality Indices, Spectral Signature and Multivariate Modeling. *Water* **2022**, *14*, 1131. [CrossRef]
29. Khadr, M.; Gad, M.; El-Hendawy, S.; Al-Suhaibani, N.; Dewir, Y.H.; Tahir, M.U.; Mubushar, M.; Elsayed, S. The Integration of Multivariate Statistical Approaches, Hyperspectral Reflectance, and Data-Driven Modeling for Assessing the Quality and Suitability of Groundwater for Irrigation. *Water* **2021**, *13*, 35. [CrossRef]
30. Eid, M.H.; Elbagory, M.; Tamma, A.A.; Gad, M.; Elsayed, S.; Hussein, H.; Moghanm, F.S.; Omara, A.E.-D.; Kovács, A.; Péter, S. Evaluation of Groundwater Quality for Irrigation in Deep Aquifers Using Multiple Graphical and Indexing Approaches Supported with Machine Learning Models and GIS Techniques, Souf Valley, Algeria. *Water* **2023**, *15*, 182. [CrossRef]
31. Schulze, F.H.; Wolf, H.; Jansen, H.W.; van der Veer, P. Applications of Artificial Neural Networks in Integrated Water Management: Fiction or Future? *Water Sci. Technol.* **2005**, *52*, 21–31. [CrossRef]
32. Strobl, C.; Boulesteix, A.-L.; Kneib, T.; Augustin, T.; Zeileis, A. Conditional Variable Importance for Random Forests. *BMC Bioinform.* **2008**, *9*, 307. [CrossRef]
33. Glorfeld, L. A Methodology for Simplification and Interpretation of Backpropagation-Based Neural Network Models. *Expert Syst. Appl.* **1996**, *10*, 37–54. [CrossRef]
34. Melis, G.; Dyer, C.; Blunsom, P. On the State of the Art of Evaluation in Neural Language Models. *arXiv* **2017**, arXiv:1707.05589.
35. Bergstra, J.; Yamins, D.; Cox, D. Making a Science of Model Search: Hyperparameter Optimization in Hundreds of Dimensions for Vision Architectures. In Proceedings of the 30th International Conference on Machine Learning, Atlanta, GA, USA, 16–21 June 2013; Dasgupta, S., McAllester, D., Eds.; Volume 28, pp. 115–123.
36. Wu, J.; Chen, X.-Y.; Zhang, H.; Xiong, L.-D.; Lei, H.; Deng, S.-H. Hyperparameter Optimization for Machine Learning Models Based on Bayesian Optimizationb. *J. Electron. Sci. Technol.* **2019**, *17*, 26–40. [CrossRef]
37. Gad, M.; El Osta, M. Geochemical Controlling Mechanisms and Quality of the Groundwater Resources in El Fayoum Depression, Egypt. *Arab. J. Geosci.* **2020**, *13*, 861. [CrossRef]

38. Gul, S.; Gul, H.; Gul, M.; Khattak, R.; Rukh, G.; Khan, M.S.; Aouissi, H.A. Enhanced Adsorption of Rhodamine B on Biomass of Cypress/False Cypress (Chamaecyparis lawsoniana) Fruit: Optimization and Kinetic Study. *Water* **2022**, *14*, 2987. [CrossRef]
39. Bencer, S.; Boudoukha, A.; Mouni, L. Multivariate Statistical Analysis of the Groundwater of Ain Djacer Area (Eastern of Algeria). *Arab. J. Geosci.* **2016**, *9*, 248. [CrossRef]
40. Eaton, A.D.; Clesceri, L.S.; Rice, E.W.; Greenberg, A.E.; Franson, A.H. (Eds.) *Standard Methods for the Examination of Water & Wastewater*, 21st ed.; Amer Public Health Association: Washington, DC, USA, 2005.
41. Gaagai, A.; Boudoukha, A.; Boumezbeur, A.; Benaabidate, L. Hydrochemical Characterization of Surface Water in the Babar Watershed (Algeria) Using Environmetric Techniques and Time Series Analysis. *Int. J. River Basin Manag.* **2017**, *15*, 361–372. [CrossRef]
42. Gad, M.; Elsayed, S.; Moghanm, F.S.; Almarshadi, M.H.; Alshammari, A.S.; Khedher, K.M.; Eid, E.M.; Hussein, H. Combining Water Quality Indices and Multivariate Modeling to Assess Surface Water Quality in the Northern Nile Delta, Egypt. *Water* **2020**, *12*, 2142. [CrossRef]
43. Belkhiri, L.; Boudoukha, A.; Mouni, L.; Baouz, T. Application of Multivariate Statistical Methods and Inverse Geochemical Modeling for Characterization of Groundwater—A Case Study: Ain Azel Plain (Algeria). *Geoderma* **2010**, *159*, 390–398. [CrossRef]
44. Hinge, G.; Bharali, B.; Baruah, A.; Sharma, A. Integrated Groundwater Quality Analysis Using Water Quality Index, GIS and Multivariate Technique: A Case Study of Guwahati City. *Environ. Earth Sci.* **2022**, *81*, 412. [CrossRef]
45. Kaiser, H.F. The Varimax Criterion for Analytic Rotation in Factor Analysis. *Psychometrika* **1958**, *23*, 187–200. [CrossRef]
46. Schoeller, H. Methods and Techniques of Groundwater Investigation and Development. *Water Resour. Ser.* **1967**, *33*, 44–52.
47. Meireles, A.C.M.; de Andrade, E.M.; Chaves, L.C.G.; Frischkorn, H.; Crisostomo, L.A. A New Proposal of the Classification of Irrigation Water. *Rev. Ciênc. Agron.* **2010**, *41*, 349–357. [CrossRef]
48. Oster, J.D.; Sposito, G. The Gapon Coefficient and the Exchangeable Sodium Percentage-Sodium Adsorption Ratio Relation. *Soil Sci. Soc. Am. J.* **1980**, *44*, 258–260. [CrossRef]
49. Srinivasamoorthy, K.; Gopinath, M.; Chidambaram, S.; Vasanthavigar, M.; Sarma, V.S. Hydrochemical Characterization and Quality Appraisal of Groundwater from Pungar Sub Basin, Tamilnadu, India. *J. King Saud Univ. Sci.* **2014**, *26*, 37–52. [CrossRef]
50. Ravikumar, P.; Aneesul Mehmood, M.; Somashekar, R.K. Water Quality Index to Determine the Surface Water Quality of Sankey Tank and Mallathahalli Lake, Bangalore Urban District, Karnataka, India. *Appl. Water Sci.* **2013**, *3*, 247–261. [CrossRef]
51. Zhang, T.; Cai, W.; Li, Y.; Geng, T.; Zhang, Z.; Lv, Y.; Zhao, M.; Liu, J. Ion Chemistry of Groundwater and the Possible Controls within Lhasa River Basin, SW Tibetan Plateau. *Arab. J. Geosci.* **2018**, *11*, 510. [CrossRef]
52. Das, S.; Nag, S.K. Deciphering Groundwater Quality for Irrigation and Domestic Purposes—A Case Study in Suri I and II Blocks, Birbhum District, West Bengal, India. *J. Earth Syst. Sci.* **2015**, *124*, 965–992. [CrossRef]
53. Elith, J.; Leathwick, J.R.; Hastie, T. A Working Guide to Boosted Regression Trees. *J. Anim. Ecol.* **2008**, *77*, 802–813. [CrossRef]
54. Schalkoff, R.J. *Artificial Neural Networks*; McGraw-Hill Higher Education: New York, NY, USA, 1997; ISBN 0-07-057118-X.
55. Haykin, S. Self-Organizing Maps. *Neural Netw. Compr. Found.* **1999**, *2*, 443–483.
56. Li, J.; Yoder, R.E.; Odhiambo, L.O.; Zhang, J. Simulation of Nitrate Distribution under Drip Irrigation Using Artificial Neural Networks. *Irrig. Sci.* **2004**, *23*, 29–37. [CrossRef]
57. Byrd, R.H.; Lu, P.; Nocedal, J.; Zhu, C. A Limited Memory Algorithm for Bound Constrained Optimization. *SIAM J. Sci. Comput.* **1995**, *16*, 1190–1208. [CrossRef]
58. Noori, R.; Karbassi, A.R.; Mehdizadeh, H.; Vesali-Naseh, M.; Sabahi, M.S. A framework development for predicting the longitudinal dispersion coefficient in natural streams using an artificial neural network. *Environ. Prog. Sustain. Energy* **2011**, *30*, 439–449. [CrossRef]
59. Zhu, J.; Huang, Z.; Sun, H.; Wang, G. Mapping Forest Ecosystem Biomass Density for Xiangjiang River Basin by Combining Plot and Remote Sensing Data and Comparing Spatial Extrapolation Methods. *Remote Sens.* **2017**, *9*, 241. [CrossRef]
60. Malone, B.P.; Styc, Q.; Minasny, B.; McBratney, A.B. Digital Soil Mapping of Soil Carbon at the Farm Scale: A Spatial Downscaling Approach in Consideration of Measured and Uncertain Data. *Geoderma* **2017**, *290*, 91–99. [CrossRef]
61. Saggi, M.K.; Jain, S. Reference Evapotranspiration Estimation and Modeling of the Punjab Northern India Using Deep Learning. *Comput. Electron. Agric.* **2019**, *156*, 387–398. [CrossRef]
62. Lakshmanan, E.; Kannan, R.; Senthil Kumar, M. Major Ion Chemistry and Identification of Hydrogeochemical Processes of Ground Water in a Part of Kancheepuram District, Tamil Nadu, India. *Environ. Geosci.* **2003**, *10*, 157–166. [CrossRef]
63. Ayers, R.; Westcott, D. *Water Quality for Agriculture. FAO Irrigation and Drainage*; Paper 29 Revision 1; Food and Agricultural Organization of the United Nations: Rome, Italy, 1994.
64. Athamena, A.; Gaagai, A.; Aouissi, H.A.; Burlakovs, J.; Bencedira, S.; Zekker, I.; Krauklis, A.E. Chemometrics of the Environment: Hydrochemical Characterization of Groundwater in Lioua Plain (North Africa) Using Time Series and Multivariate Statistical Analysis. *Sustainability* **2023**, *15*, 20. [CrossRef]
65. Gaagai, A.; Aouissi, H.A.; Krauklis, A.E.; Burlakovs, J.; Athamena, A.; Zekker, I.; Boudoukha, A.; Benaabidate, L.; Chenchouni, H. Modeling and Risk Analysis of Dam-Break Flooding in a Semi-Arid Montane Watershed: A Case Study of the Yabous Dam, Northeastern Algeria. *Water* **2022**, *14*, 767. [CrossRef]
66. Ghalib, H.B. Groundwater Chemistry Evaluation for Drinking and Irrigation Utilities in East Wasit Province, Central Iraq. *Appl. Water Sci.* **2017**, *7*, 3447–3467. [CrossRef]

67. Tang, H.; Zhong, H.; Pan, Y.; Zhou, Q.; Huo, Z.; Chu, W.; Xu, B. A New Group of Heterocyclic Nitrogenous Disinfection Byproducts (DBPs) in Drinking Water: Role of Extraction PH in Unknown DBP Exploration. *Environ. Sci. Technol.* **2021**, *55*, 6764–6772. [CrossRef]
68. Selvam, S.; Venkatramanan, S.; Chung, S.Y.; Singaraja, C. Identification of Groundwater Contamination Sources in Dindugal District of Tamil Nadu, India Using GIS and Multivariate Statistical Analyses. *Arab. J. Geosci.* **2016**, *9*, 407. [CrossRef]
69. Litvinovich, A.; Pavlova, O.; Lavrishchev, A.; Bure, V.; Saljnikov, E. Magnesium Leaching Processes from Sod-Podzolic Sandy Loam Reclaimed by Increasing Doses of Finely Ground Dolomite. *Zemdirb. Agric.* **2021**, *108*, 109–116. [CrossRef]
70. Guerzou, M.; Aouissi, H.A.; Guerzou, A.; Burlakovs, J.; Doumandji, S.; Krauklis, A.E. From the Beehives: Identification and Comparison of Physicochemical Properties of Algerian Honey. *Resources* **2021**, *10*, 94. [CrossRef]
71. Piper, A.M. A Graphic Procedure in the Geochemical Interpretation of Water-Analyses. *Trans. AGU* **1944**, *25*, 914. [CrossRef]
72. Alqarawy, A.; El Osta, M.; Masoud, M.; Elsayed, S.; Gad, M. Use of Hyperspectral Reflectance and Water Quality Indices to Assess Groundwater Quality for Drinking in Arid Regions, Saudi Arabia. *Water* **2022**, *14*, 2311. [CrossRef]
73. Gibbs, R.J. Mechanisms Controlling World Water Chemistry. *Science* **1970**, *170*, 1088–1090. [CrossRef]
74. Ghahremanzadeh, H.; Noori, R.; Baghvand, A.; Nasrabadi, T. Evaluating the main sources of groundwater pollution in the southern Tehran aquifer using principal component factor analysis. *Environ. Geochem. Health* **2018**, *40*, 1317–1328. [CrossRef]
75. Wu, J.; Li, P.; Qian, H. Hydrochemical Characterization of Drinking Groundwater with Special Reference to Fluoride in an Arid Area of China and the Control of Aquifer Leakage on Its Concentrations. *Environ. Earth Sci.* **2015**, *73*, 8575–8588. [CrossRef]
76. Mukherjee, A.; Fryar, A.E.; Scanlon, B.R.; Bhattacharya, P.; Bhattacharya, A. Elevated Arsenic in Deeper Groundwater of the Western Bengal Basin, India: Extent and Controls from Regional to Local Scale. *Appl. Geochem.* **2011**, *26*, 600–613. [CrossRef]
77. Diwakar, J.; Johnston, S.G.; Burton, E.D.; Shrestha, S.D. Arsenic Mobilization in an Alluvial Aquifer of the Terai Region, Nepal. *J. Hydrol. Reg. Stud.* **2015**, *4*, 59–79. [CrossRef]
78. Kumar, S.; Kumar, A.; Prashant; Jha, V.N.; Sahoo, S.K.; Ranjan, R.K. Groundwater Quality and Its Suitability for Drinking and Irrigational Purpose in Bhojpur District: Middle Gangetic Plain of Bihar, India. *Water Supply* **2022**, *22*, 7072–7084. [CrossRef]
79. Islam, J.; Hossain, A.M.; Rahman, S.; Khandoker, H.; Zahan, M.N. Hydrogeochemistry and Usability of Groundwater at the Tista River Basin in Northern Bangladesh. *Indian J. Sci. Technol.* **2019**, *12*, 1–12. [CrossRef]
80. Qian, C.; Wu, X.; Mu, W.-P.; Fu, R.-Z.; Zhu, G.; Wang, Z.-R.; Wang, D. Hydrogeochemical Characterization and Suitability Assessment of Groundwater in an Agro-Pastoral Area, Ordos Basin, NW China. *Environ. Earth Sci.* **2016**, *75*, 1356. [CrossRef]
81. Noori, R.; Berndtsson, R.; Hosseinzadeh, M.; Adamowski, J.F.; Abyaneh, M.R. A critical review on the application of the National Sanitation Foundation Water Quality Index. *Environ. Pollut.* **2019**, *244*, 575–587. [CrossRef]
82. Güler, C.; Thyne, G.D.; McCray, J.E.; Turner, K.A. Evaluation of Graphical and Multivariate Statistical Methods for Classification of Water Chemistry Data. *Hydrogeol. J.* **2002**, *10*, 455–474. [CrossRef]
83. Kawo, N.S.; Karuppannan, S. Groundwater Quality Assessment Using Water Quality Index and GIS Technique in Modjo River Basin, Central Ethiopia. *J. Afr. Earth Sci.* **2018**, *147*, 300–311. [CrossRef]
84. Li, P.; Wu, J.; Qian, H. Assessment of Groundwater Quality for Irrigation Purposes and Identification of Hydrogeochemical Evolution Mechanisms in Pengyang County, China. *Environ. Earth Sci.* **2013**, *69*, 2211–2225. [CrossRef]
85. Noori, R.; Hooshyaripor, F.; Javadi, S.; Dodangeh, M.; Tian, F.; Adamowski, J.F.; Berndtsson, R.; Baghvand, A.; Klöve, B. PODMT3DMS-Tool: Proper orthogonal decomposition linked to the MT3DMS model for nitrate simulation in aquifers. *Hydrogeol. J.* **2020**, *28*, 1125–1142. [CrossRef]
86. RamyaPriya, R.; Elango, L. Evaluation of Geogenic and Anthropogenic Impacts on Spatio-Temporal Variation in Quality of Surface Water and Groundwater along Cauvery River, India. *Environ. Earth Sci.* **2018**, *77*, 2. [CrossRef]
87. Elsayed, S.; Ibrahim, H.; Hussein, H.; Elsherbiny, O.; Elmetwalli, A.H.; Moghanm, F.S.; Ghoneim, A.M.; Danish, S.; Datta, R.; Gad, M. Assessment of Water Quality in Lake Qaroun Using Ground-Based Remote Sensing Data and Artificial Neural Networks. *Water* **2021**, *13*, 3094. [CrossRef]
88. Wang, X.; Ozdemir, O.; Hampton, M.A.; Nguyen, A.V.; Do, D.D. The Effect of Zeolite Treatment by Acids on Sodium Adsorption Ratio of Coal Seam Gas Water. *Water Res.* **2012**, *46*, 5247–5254. [CrossRef]
89. Hanson, B.; Grattan, S.R.; Fulton, A. *Agricultural Salinity and Drainage*; Irrigation Program, University of California: Davis, CA, USA, 1999.
90. Sudhakar, A.; Narsimha, A. Suitability and Assessment of Groundwater for Irrigation Purpose: A Case Study of Kushaiguda Area, Ranga Reddy District, Andhra Pradesh, India. *Adv. Appl. Sci. Res.* **2013**, *4*, 75–81.
91. Kelley, W.P. Permissible Composition and Concentration of Irrigation Water. *Proc. Am. Soc. Civil Eng.* **1940**, *66*, 607–613. [CrossRef]
92. Sundaray, S.K.; Nayak, B.B.; Bhatta, D. Environmental Studies on River Water Quality with Reference to Suitability for Agricultural Purposes: Mahanadi River Estuarine System, India—A Case Study. *Environ. Monit. Assess.* **2009**, *155*, 227–243. [CrossRef]
93. Todd, D.K.; Mays, L.W. *Groundwater Hydrology*; John Wiley & Sons: Hoboken, NJ, USA, 2004; ISBN 0-471-05937-4.
94. Wilcox, L.V. *The Quality of Water for Irrigation Use*; Technical Bulletin; US Government Printing Office: Washington, DC, USA, 1948; 19p.
95. Paliwal, K.V. *Irrigation with Saline Water*; Water Technology Centre, Indian Agriculture Research Institute: New Delhi, India, 1972.
96. Doneen, L.D. *Water Quality for Agriculture, Department of Irrigation*; University of California: Davis, CA, USA, 1964; p. 48.

97. Elsherbiny, O.; Zhou, L.; Feng, L.; Qiu, Z. Integration of Visible and Thermal Imagery with an Artificial Neural Network Approach for Robust Forecasting of Canopy Water Content in Rice. *Remote Sens.* **2021**, *13*, 1785. [CrossRef]
98. Elsherbiny, O.; Zhou, L.; He, Y.; Qiu, Z. A Novel Hybrid Deep Network for Diagnosing Water Status in Wheat Crop Using IoT-Based Multimodal Data. *Comput. Electron. Agric.* **2022**, *203*, 107453. [CrossRef]